



GEOLOGICAL SURVEY OF CANADA

OPEN FILE 2277

This document was produced
by scanning the original publication.

Ce document a été produit par
numérisation de la publication originale.

**Mineralogical and petrological studies
of the Crystal Lake Intrusion,
Thunder Bay, Ontario**

Ersen H. Cogulu

1990



Energy, Mines and
Resources Canada

Énergie, Mines et
Ressources Canada

Canada



Contribution to Canada-Ontario 1985 Mineral Development
Subsidiary Agreement under the Economic and Regional
Development Agreement. Project funded by the Geological
Survey of Canada.



Energy, Mines and
Resources Canada

Énergie, Mines et
Ressources Canada



GEOLOGICAL SURVEY OF CANADA

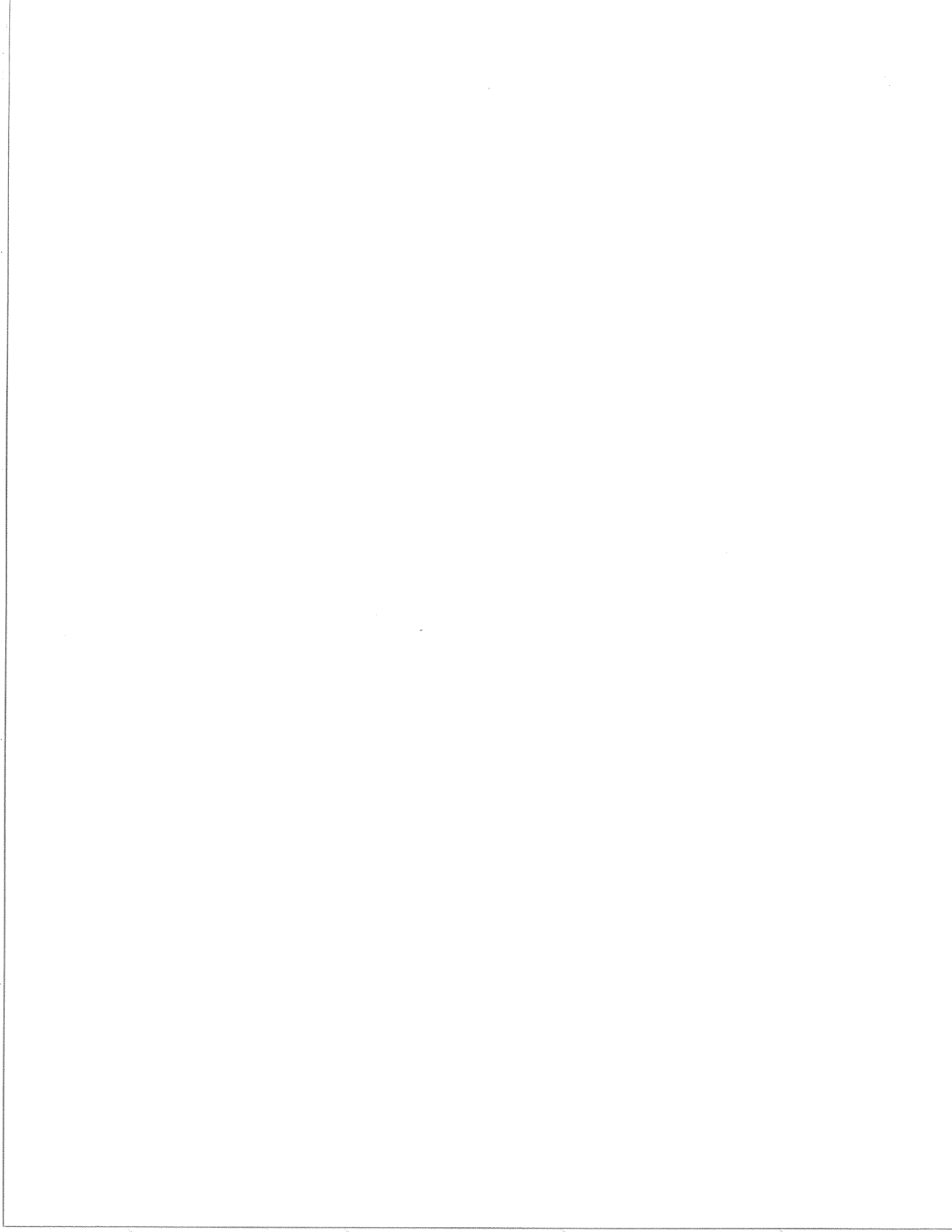
OPEN FILE 2277

**Mineralogical and petrological studies
of the Crystal Lake Intrusion,
Thunder Bay, Ontario**

Ersen H. Cogulu

Report submitted under the terms
of DSS contract no. 34SZ.23233-7-760
Canada-Ontario Mineral Development Agreement

1990



ABSTRACT

The Crystal Lake Intrusion located northwest of Lake Superior, Ontario, is one of the multiple intrusions related to intracontinental rifting of Proterozoic age. It exhibits trough shaped layering and four stratigraphic zones. The Basal Zone representing the chilled margin of the intrusion is contaminated by sedimentary country rocks and contains numerous xenoliths and sulphide mineralization. The Lower Unlayered Zone hosts the major portion of the low grade copper-nickel mineralization known as the Great Lakes Nickel deposit, and consists of three structural subzones. The Cyclic Zone comprises four repetitive sequences formed by periodic influx of magma, and contains chrome spinel, Cu-Ni sulphide and platinum group element mineralization. The cyclic units contain the most differentiated rocks of the intrusion. Chrome spinel bearing layers exhibit soft sediment-like deformation. The Upper Zone composed of unlayered massive gabbros indicates return to magmatic conditions that produce undifferentiated rocks.

Orthocumulate rocks are dominant in the Crystal Lake intrusion. Adcumulates occur only in the cyclic zone in association with chrome spinel mineralization. Plagioclase is the main cumulus mineral, which forms the framework of the rocks. Olivine is locally cumulus and indicates new magma influx; in most cases it is reequilibrated with trapped intercumulus liquid. Augite is always intercumulus and may be the product of transformation of olivine.

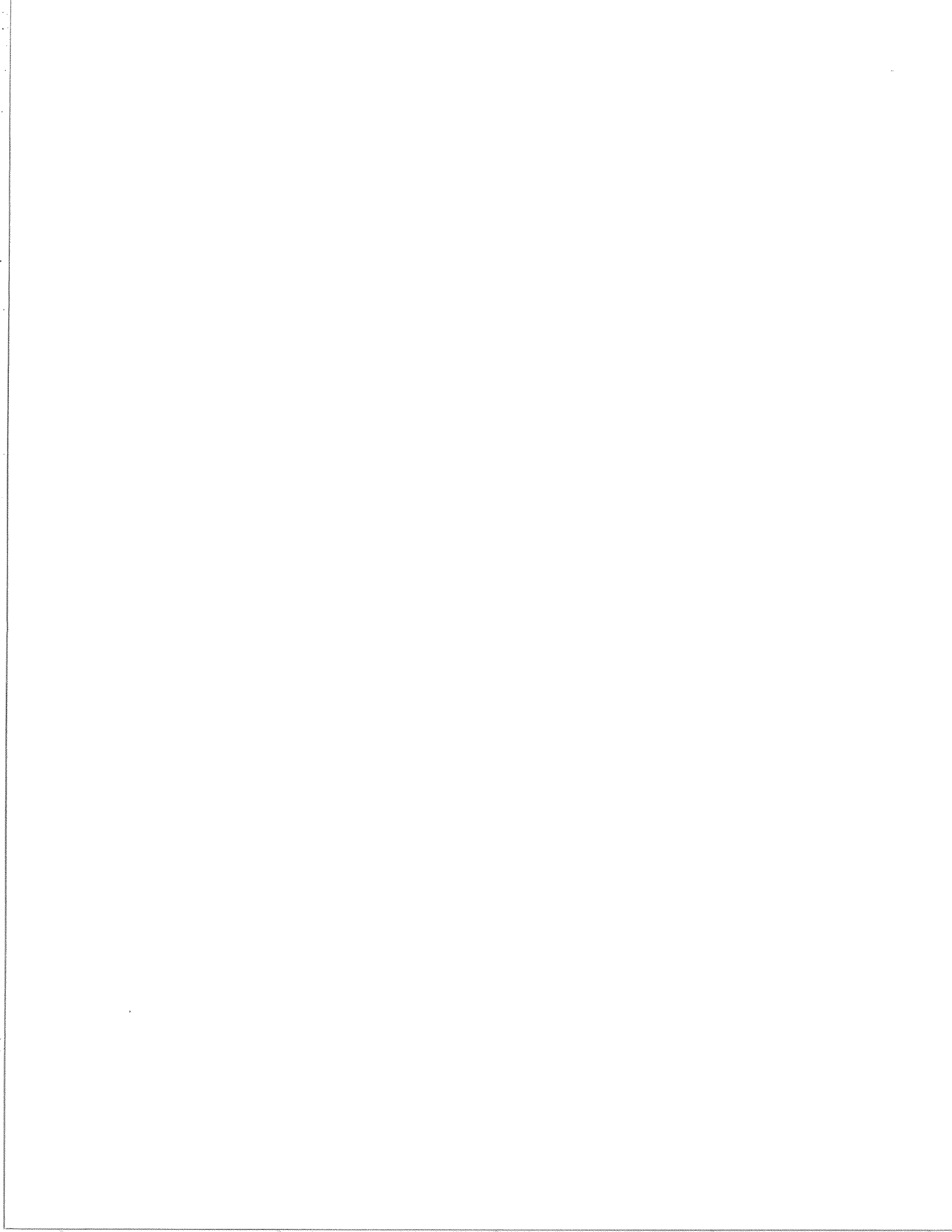
Biotite is epitaxial to olivine and augite; it may also rim intercumulus sulphide and oxides. The total REE concentrations decrease from the basal zone to the cyclic sequence and are accompanied by decreasing LREE/HREE ratios. The cyclic unit gabbros exhibit positive Eu anomalies that are not observed in the lower zones. Partial melting and dehydration of the country rock gave rise to contamination of the magma. Partial melting and contamination of major elements are restricted to the basal zone as well as to areas near the sedimentary xenoliths in the lower unlayered zone. There is no evidence of contamination of the cyclic units.

I INTRODUCTION

The Crystal Lake intrusion is located northwest of Lake Superior in Ontario, a few kilometres from the Canada-Minnesota international boundary (Fig.1). It is made up of gabbroic rocks, and is genetically related to the Duluth Complex in Minnesota. The latter is a composite body of multiple intrusions emplaced approximately 1.1 Ga years ago (Silver and Green, 1972). The Duluth magmatism and associated Keweenaw volcanism are considered to be related to the rift zone that is expressed geophysically as the Mid-Continent gravity high (Chase and Gilmer, 1973: Fig.1). The Crystal Lake gabbros were intruded during this same period of crustal extension (Weiblen, 1982).

The Crystal Lake intrusion was the focus of exploration interest during the 1960s and 1970s because of the presence of disseminated Cu-Ni sulphides. It was tested by an intensive drilling program in order to assess its Cu-Ni potential. On the basis of drill core examination the intrusion was subdivided into three zones (Reeve, 1969; Geul, 1970): 1) an upper zone consisting of medium grained olivine gabbro; 2) a middle "pegmatitic" zone containing sulphide mineralization and chromitite bands marking its upper limit; and 3) a basal or chill zone containing dark, medium to fine grained gabbros and sulphides. Cogulu (1984, 1985) recognized the presence of a cyclically layered zone anomalous in platinum group elements (PGE). This finding caused a resurgence of interest and the PGE potential of the cyclic zone was tested in 1986.

The purpose of this paper is to document geological, petrological and chemical characteristics of the intrusion with a view to explaining the formation of sulphide, chromite and platinum group elements mineralization, and the role of country rock contamination.



II REGIONAL GEOLOGY

The Keweenaw intrusive rocks occurring in the Lake Superior region are subdivided into three groups by Weiblen (1982): 1) layered tholeiitic intrusions, 2) dyke and sill swarms of quartz- and olivine-tholeiite affinities, and 3) alkaline intrusions. The first and second groups are represented in the study area (Fig.2 and 3).

The Crystal Lake region is underlain by strata of the Animikian Rove Formation which consist of argillites, shales and greywackes. These rocks were intruded by diabasic sills and dykes as well as by the Crystal Lake gabbros (Geul, 1970). The Logan sills and Pigeon River dykes are topographically prominent and form the main cuestas and ridges of the region. The Logan Sills are the earlier intrusions and occur as flat to gently dipping sheets quasiconformable with the sedimentary rocks. The Pigeon River dykes form an east to northeast trending swarm (Fig.2). Detailed field examination during the present study revealed complex relationships between dykes, sills and gabbros. The main observations are the following: a) dykes may be intruded into each other in similar manner to those in ophiolitic suites. This is the main evidence of tensional conditions which controlled their emplacement; b) Some sills and dykes crosscut each other indicating they are contemporaneous; c) The Crystal Lake intrusion crosscuts most of the dykes, but in turn it was crosscut by others as observed in drill core and northeast of Bearpad Lake (Fig.2). This demonstrates that dyke emplacement started prior to the intrusion of the Crystal Lake gabbros and continued afterward.

The Crystal lake intrusion outcrops as a "Y" shaped body (Fig.2). Its northern arm which hosts the Great Lakes Nickel (GLN) deposit extends for about 6 km in a west-northwest direction. The southern arm is parallel to Pigeon River dikes and extends for about 2 km (Geul, 1970).

III SAMPLING AND ANALYTICAL METHODS

Approximately 250 rock samples were collected from outcrops and drill core. 200 thin and polished thin sections were examined microscopically in reflected and transmitted light. 500 electronic microprobe analyses were performed on silicate minerals. The analyses are classified according to structural zones and given in Tables 4 to 11.

Two different microprobe analysers were used: 1) an MAC electron microprobe equipped with a Kevex energy dispersive spectrometer at the Geological Survey of Canada, Ottawa was operated at 20 KV acceleration voltage, a specimen current of 10 nA, and a counting time of 100 seconds. 2) a Cambridge Mark V electron microprobe at Dalhousie University, Department of Geology, Halifax was operated at 15 KV acceleration potential and a beam current of 5 nA. The Ortex energy dispersive system has a detector resolution of 149 EV. The software package used was EDATA 2 (Smith et al. 1980). Rare earth element analyses were performed by neutron activation at Nuclear Activation Services Ltd., McMaster University. Whole rock analyses for major and trace elements were done by XRF at X-Ray Assay Laboratories, Toronto and at the Department of Geology, University of Ottawa.

The terminology used in this paper relating to cumulate rocks does not imply settled crystals and follows that of Irvine (1982).

IV INTERNAL STRATIGRAPHY OF THE INTRUSION.

The Crystal Lake intrusion has not been metamorphosed and only slightly altered, and so the mineral assemblages have not been changed. The basal zone of the intrusion is not exposed, but drill holes penetrated the sedimentary country rocks which display thermal metamorphism. Part of the internal stratigraphy of the northern arm is exposed in the western cliffs which provide a natural north-south cross section of the intrusion. Layering is visible in the upper half of the cliffs and consists mainly of alternating anorthositic gabbro and olivine gabbro. The layers form a trough with the northern flank dipping to the south more steeply than the south flank dips to the north. The trough plunges 15-20° to the east.

The Crystal Lake intrusion is made up of cumulate rocks. Orthocumulate rocks are dominant, but adcumulate layers also are observed. Plagioclase and olivine are the two main cumulus silicates. Chrome spinel occurs only in the cyclic zone. Clinopyroxene, hornblende, biotite, orthopyroxene, apatite, ilmenite and sulphides are intercumulus.

Four stratigraphic zones are distinguished in the western portion of the intrusion (Fig. 4). They are, in stratigraphically descending order, the following:

1) The Upper Zone has a thickness of about 60 m in the western cliffs and thickens to the East. It mainly consists of medium grained alternating troctolite, olivine gabbro, and anorthositic gabbro. This is modally and texturally the most homogeneous zone in the intrusion. Modal abundances of plagioclase and olivine are 56-70% and 18-23% respectively. The modal proportions of the interstitial material are up to 17% of augite, about 1% of biotite, and 1-2 % of oxide.

2) Cyclic Zone. Four magmatic cycles constitute a distinct layered sequence between the upper zone and lower unlayered Cu-Ni mineralized zone. Its total thickness attains 42 m above the upper adit. The cyclic zone differs from the other zones in its mineral and rock constituents, and anomalous content of chromite and PGE. The latter mineralization occurs in the lower and middle portions of cycles whereas the anorthositic gabbros lie in the upper portions of the cyclic units.

3) The Lower Unlayered Zone (LUZ) contains the major part of the Cu-Ni mineralization (Great Lakes Nickel deposit). The main rock type is a massive gabbro which is characterized by variable textures ranging from fine grained to pegmatitic. Sulphide disseminations are scattered throughout, but more often in the pegmatitic patches. Cognate and sedimentary xenoliths are common, the latter increasing in abundance with the depth.

4) The Basal Zone does not outcrop in the field, but drill core shows fine-grained, dark colored gabbros at the base of the intrusion. The thickness of the basal zone varies between 1 and 6 m, but locally it may be thicker, and contains numerous hornfels xenoliths. Sulphides form scattered disseminations, drop-like blebs, and massive lenses or stringers. Sediments are transformed into hornfels adjacent to their contact with the intrusion. Felsic material forming anastomosing veins is common in basal and hornfels zone. The increase of felsic material may locally form mixed rocks.

V MINERALOGY AND PETROGRAPHY OF THE ZONES

In the following sections the basal, lower unlayered and cyclic zones are described in detail. These observations as well as analytical data are mainly based on surface samples from the western cliffs of the northern arm, and core samples from drill hole DH-18 (drilled from the upper adit, representing the unexposed portion of the intrusion below the western cliffs; Fig.5).

V.1 BASAL ZONE

The main rock type is a plagioclase orthocumulate. The plagioclase occurs commonly as small, randomly oriented, sericitized tabular crystals, and forms the main framework for intercumulus minerals. Olivine is not observed in the basal zone. Augite is interstitial and forms poikilitic and skeletal oikocrysts which are often transformed into chlorite. Orthopyroxene may form euhedral to subhedral poikilitic crystals. The modal proportions of pyroxenes are higher than those in the overlying zones. Coarser grained felsic material fills anastomosing veins or interstices between cumulus plagioclase, and is composed of quartz, orthoclase, acid plagioclase and biotite. The two first minerals commonly form micrographic and granophyric textures surrounding euhedral plagioclases. The basal zone rocks are richer in biotite than those in the other zones. On the basis of occurrence and composition two types of biotite are recognised (Fig.6; Table 5). The first is interstitial or epitaxial to augite, and it is richer in Mg and poorer in Fe and Ti. The second is associated with felsic material, and commonly contains zircon inclusions surrounded by pleochroic halos; it is richer in Fe and Ti and depleted in Mg.

V.2 LOWER UNLAYERED ZONE (LUZ)

The major portion of the lower unlayered zone (LUZ) is hidden from view. The only location where it outcrops is the west face of the northern arm where its upper 20 m portion is exposed (Fig.5). The LUZ has a concave-up shape in North-South cross-section, and its thickness decreases toward the margins. One km to the East its thickness reaches 200 m in the keel zone. The LUZ is divisible into three sub-units, A, B, and C from the bottom upward, on the basis of rock types and cryptic variations of mafic minerals (Fig.7).

V.2.A Petrography

The LUZ is composed of gabbros ranging in grain size from fine to very coarse. Pegmatitic material having compositions ranging from olivine gabbro to anorthositic gabbro forms irregular patches surrounded by fine to medium grained material. The grain size and proportion of gabbroic pegmatites increases upward. Cognate xenoliths are common and particularly abundant in the upper portion of the LUZ in the vicinity of the upper adit. Sedimentary xenoliths are sparsely distributed and transformed into hornfels. Sulphides form disseminations which are preferentially located in coarse grained gabbros.

Three rock types are recognised: plagioclase-olivine orthocumulate, plagioclase orthocumulate, and olivine orthocumulate (Table 1).

PLAGIOCLASE is the most abundant silicate and its modal content ranges from about 50 % to 70 % of the rock. It presents various textural forms, but commonly is found as euhedral to irregular laths which form a framework for olivine and other intercumulus material. Locally planar lamination of plagioclase may be observed. Two generations of plagioclase are distinguished. Early plagioclase has discontinuous patchy compositional zoning and may form tabular to irregular crystals in fine to medium grained gabbros. Its An content varies in general between 82 and 70 %. Later generation plagioclase is always normally zoned. It generally resorbs and surrounds the earlier plagioclase (Photos 1 to 4). Late plagioclase also forms tabular to irregular crystals in medium grained to pegmatitic gabbros. Its An content is however lower and ranges from about 70 to 30 %.

OLIVINE is the second most abundant silicate, and it comprises from 3 to 25 % of the rock. It exhibits four textural forms: equant euhedral to rounded, poikilitic, interstitial, and relicts in augite. As indicated by these different morphologies olivine may crystallize prior to, simultaneously with, and after the plagioclase. Euhedral to rounded olivine grains are found in olivine orthocumulates at the base of the Unit B. In other rocks olivines are always intercumulus and form oikocrysts. In general, olivines resorb patchy zoned plagioclases, and exhibit intergrowth textures with normal zoned ones (Photo 2,6 and 7). Poikilitic olivines may contain partly resorbed plagioclase relicts and display triple joint contact. Skeletal olivines commonly exhibit upward branching (Photo 8). These relationships to plagioclase may indicate a genetic sequence in which olivine is contemporaneous with, and later than plagioclase. Fo content of olivines ranges from 69 to 53 %. The interstitial skeletal olivines are more fayalitic than the poikilitic ones. The pegmatitic olivine forms large amoeboidal and zoned crystals which are intergrown with later plagioclases (Photo 6). They have a wide range of Fo content, 44 to 63 %.

AUGITE is the most abundant intercumulus mineral, constituting between 2 and 18 % of the rock. It forms poikilitic to interstitial large oikocrysts. Poikilitic augite exhibits textural relationships with plagioclase similar to those of olivine. It often contains embayed plagioclase and relicts of olivines (Photo 13 and 14). Numerous augites contain olivine relicts, and display optic orientation related to that of the relict olivine. These relationships may indicate that augite crystallized from the reaction of olivine with intercumulus liquid. Sulphides are often included in augite as eutectoid-like blebs (Photo 1 and 16). Composition of augite vary depending upon textural form and sulphide inclusions. Those containing sulphides are richer in iron (Fig.8). Mg number of augites correlates with those of olivine in given samples (Fig.7). Poikilitic augite which contains plagioclase relicts has higher Mg numbers than interstitial augite.

ORTHOPYROXENE is less abundant than augite and occurs only as an accessory mineral. It presents two textural forms in two different rocks. In pegmatitic gabbro orthopyroxene occurs in a symplectite intergrowth with plagioclase at the margins of olivine (Photo 15). In fine to medium grained gabbro it is epitactic to olivine.

BIOTITE occurs in small amounts in three textural forms: 1) epitactic to olivine, it is associated with orthopyroxene and ilmenite in the pegmatitic gabbro. 2) epitactic to augite, it is commonly observed in all samples. 3) interstitial biotite commonly rims sulphides and oxides.

HORNBLLENDE occurs in accessory amounts in pegmatitic gabbro as epitaxial overgrowths to augite.

CI-APATITE commonly occurs as small prisms disseminated within sulphides and biotite.

ILMENITE is the main oxide and forms irregular to skeletal crystals in pegmatitic and medium grained gabbros.

SULPHIDES present are generally a monoclinic pyrrhotite-chalcopyrite-cubanite-pentlandite assemblage. Locally the pyrrhotite may be hexagonal. Monoclinic pyrrhotite is dominant in the lower portion of the ULZ and basal zone. Sulphides occurs in many textural forms: interstitial to the silicate framework, as symplectic intergrowths with orthopyroxene, as eutectoid-like inclusions within augite, etc. (Cogulu, 1988a).

V.2.B Sub-units.

The recognition of three sub-units is based on textural and compositional variations of mafic silicates. The contacts between them are gradational (Fig.7).

The lowermost Sub-unit A overlies the basal zone. It comprises mainly fine grained gabbro with a few coarser patches. The plagioclase laths may exhibit planar lamination and patchy zoning. The olivine is equant and rounded, and also forms bleb-like intergrowth textures with plagioclase at the base of the Sub-unit A (Photo 7). The olivine grades to poikilitic to interstitial skeletal oikocrysts upward in the Unit. The clinopyroxene also, forms poikilitic to interstitial oikocrysts similar to those of the olivine. A minor amount of biotite is epitactic to clinopyroxene.

Sub-unit B is separated from sub-unit A by an olivine-orthocumulate rock in which the olivine occurs as a cumulus mineral. It forms equant euhedral crystals (Fig.5). The crystallization of cumulus olivine may indicate the emplacement of a new batch of magma. Medium grained gabbro is dominant in sub-unit B, but the abundance of pegmatitic material increases in the upper portion. The plagioclase laths exhibit both patchy and normal zoning, and locally exhibit planar lamination. The euhedral olivine gives way upward to poikilitic to interstitial skeletal oikocrysts. The clinopyroxene is also poikilitic to interstitial, and forms large oikocrysts. In the middle portion of sub-unit B, felsic intercumulus patches composed of quartz, orthoclase, acid plagioclase, and displaying granophyric textures similar to those described in the Basal zone are locally observed. The presence of this material is attributed to the partial melting of sedimentary xenoliths which would occur in that area (see below).

The uppermost sub-unit, C, is partly exposed at the base of the western cliffs. The textural characteristics of these gabbros do not differ greatly from the underlying ones. The main features of the Unit C are a) abundant cognate xenoliths which exhibit internal layering, commonly cemented by b) abundant pegmatitic material. The size of the plagioclase may reach 5 cm in pegmatites. Compositions of augites in cognate xenoliths and surrounding pegmatite are shown in Fig.8.

V.2.C Mineral Chemistry

Compositions of the major silicates (olivine, plagioclase and augite) were determined by electron microprobe, and analyses are given in Tables 6, 7, and 8.

Plagioclase does not exhibit any distinctive variation pattern with depth. In Fig.7 compositions of olivine and augite are plotted versus depth. The diagrams show minimum and maximum Mg numbers of the minerals as well as the averages in given samples.

These diagrams demonstrate that olivine and augite compositions correlate well, and each unit presents different variation trends. Sub-unit A is characterised by iron enrichment of mafic minerals at its base. The olivine has 53% Fo while Mg number of the augite is 68 at the base of sub-unit A. Fo content of the olivine increases upward to 64 %, then it decreases again toward the base of overlying sub-unit B. At the base of sub-unit B, euhedral cumulus olivine has 64% Fo. Poikilitic to interstitial olivine in the middle and upper portion of sub-unit B shows a decreasing Fo trend. The presence of numerous cognate xenoliths within the upper part of sub-unit C disturbs the cryptic compositional pattern of the silicates, but in contrast to Unit B, the mafic minerals exhibit an enrichment in Mg toward the overlying cyclic zone.

V.3 CYCLIC ZONE

V.3.A Rock Types and Textures

The cyclic zone is more varied in minerals and rock types than the other zones. In addition to sulphides it contains chrome spinel and anomalous amounts of Platinum Group Elements (PGE). The rocks are mostly medium grained, but pegmatites are widely scattered and may locally attain one metre in thickness. Chrome spinel-bearing rocks exhibit adcumulate and orthocumulate textures whereas gabbros which do not contain spinel are mostly orthocumulate textured. Lithologic and textural varieties in the cyclic zone are summarized in Table 2.

ADCUMULATES. Two types of adcumulate textures are observed: poikilitic chrome spinel adcumulate and poikilitic olivine-chrome spinel adcumulate, alternating with each other in most cases. The modal proportion of the chrome spinel ranges from about 15% to 36%. It forms euhedral to subhedral, rounded, and sintered crystals, all poikilitically included within silicates. Its size ranges from 13 to 300 microns. Olivine makes up 14-18% as euhedral to irregular crystals of 1 to 6 mm size. Plagioclase form large laths up to 10 mm and constitutes 40-45% of the rock. It may present a weak crystal zoning. Augite and biotite occur interstitially in accessory amounts. Augite is not observed within the chrome spinel poikilitic adcumulates. Sulphides when present form interstitial grains between silicates.

ORTHOCUMULATES. Four orthocumulate assemblages are recognized: olivine-chrome spinel (osC), plagioclase-olivine-chrome spinel (posC), plagioclase-olivine (poC), and plagioclase (pC) (Table 2). Cumulus chrome spinels are poikilitically included in cumulus and intercumulus silicates.

The poikilitic olivine-chrome spinel orthocumulate is made up of about 55% olivine, 30% plagioclase, 8% augite, and 5% chrome spinel. The olivine occurs as 0.1-0.5 mm euhedral crystals. Chrome spinel forms euhedral to irregular crystals. Augite is interstitial to olivine and plagioclase. It forms oikocrysts up to 4 mm in size containing numerous cumulus olivine grains. The plagioclase exhibits patchy zoned tabular and irregular 1 mm crystals. Sulphides are interstitial to olivine. They often display curved boundaries. Biotite and orthopyroxene occur in accessory amounts.

Poikilitic plagioclase-olivine-chrome spinel orthocumulates have an average modal composition of 65% plagioclase, 15% olivine, 10% augite, 8% chrome spinel, and 1% biotite. Plagioclase forms normal zoned tabular and irregular crystals up to 4-5 mm. Olivine occurs mostly as large oikocrysts up to 4 mm. It often exhibits intergrowth textures with plagioclase (Photo 11 and 12). Chrome spinel forms euhedral to rounded crystals in cumulus silicates, sintered to irregular crystals in intercumulus material. Augite is interstitial and forms large oikocrysts. Biotite is interstitial, and may rim or include sulphides and oxides. It is also epitactic to augite. Sulphides exhibit various textural forms; they are mostly interstitial to plagioclase framework, or included within augite. They may also form polarity textured blebs in which chalcopyrite occupies the top of the bleb, and pyrrhotite the bottom, and thus serve as geopetal indicators. Ilmenite forms exsolution lamellae within large irregular chrome spinels, or occurs as skeletal crystals.

The chrome spinel free orthocumulates differ texturally from the gabbros described above by the abundance of the patchy zoned plagioclase which locally may show planar laminations. The high An patches are partially sericitized. Interstitial and skeletal olivine may locally form upwardly elongated crystals. Irregular or skeletal ilmenite is the main oxide phase of these rocks.

The pegmatitic gabbros are plagioclase orthocumulates. The plagioclase is tabular and normal zoned. Olivine commonly forms large oikocrysts which embay plagioclase. Augite may locally resorb plagioclase, but it is mostly interstitial and forms elongated oikocrysts. Orthopyroxene is intercumulus and epitactic to olivine in association with ilmenite and biotite. Hornblende is locally epitactic to augite in association with the biotite. Ilmenite forms large skeletal crystals.

The anorthositic gabbros are plagioclase orthocumulates. The plagioclase is tabular or irregular and always shows patchy zoning. The olivine forms large skeletal oikocrysts. Augite occurs as large interstitial oikocrysts; it may contain epitactic orthopyroxene and biotite. Ilmenite is irregular and skeletal.

XENOLITHS. Different types of cognate xenoliths are distinguished depending upon their texture and the presence of chrome spinel (Table 2). The chrome spinel bearing cognate xenoliths are adcumulate textured and exhibit similar petrographic characteristics to the rock described above. The chrome spinel free cognate xenoliths are fine or medium grained plagioclase-olivine orthocumulates. The cumulus plagioclase occurs as thin laths, 0.1-2 mm long, strongly zoned and commonly displaying planar laminations. Cumulus olivine forms equant euhedral crystals ranging from 0.1 to 0.5 mm. Augite and biotite are interstitial. Ilmenite occurs as irregular grains.

V.3.B Outcrop descriptions of Cyclic Units

The cyclic zone is transition between the unlayered lower zone and the layered upper zone. The layering is poor in the lowest cycle, becomes visible in the third cycle, and well developed in the fourth cycle. In the first three cycles the layers are disrupted in the manner of soft sediment deformation. Disrupted structures similar to those described by Scoates (1983) and Scoates et al. (1986) in the Bird River sill, and by Stewart (1963) in the Torridonian sandstones are shown in Fig.9. The intensity of the deformation increases downward in the zone. Each cycle exhibits characteristic deformation types (Table 3). The boundaries between cycles are gradational. Cumulus chrome spinel and olivine are used to define the bases of the cycles.

CYCLE 4 is 9 m thick and comprises seven chrome spinel rich bands alternating with olivine gabbro, anorthositic gabbro and pegmatite layers. Cross laminations and trough banding are locally well developed. The lowest two chrome spinel bands occurs in a magmatic trough 1 m above the base of the cycle. The exposed portion of the trough is 1.20 m in strike length and 35 cm deep; it is capped by the third chrome-spinel band which extends for a few meters before pinching out. The latter is overlain by a pegmatite layer 22 cm thick. Liquid escape structures are observed at the base of the trough. The fourth adcumulate chrome spinel layer is about 10 cm thick and presents load casts structures. A 50 cm thick olivine gabbro layer is intercalated between the fourth and fifth spinel layer. The adcumulate textured fifth spinel layer varies greatly in thickness over a short distance, and pinches out locally. Its lower surface presents numerous lobate bulges, from a few mm to a few cm across. A 6 cm thick chrome spinel orthocumulate layer which overlies the fifth layer is upwardly succeeded by a spinel free plagioclase-olivine orthocumulate of 2 m thickness displaying numerous cross laminations. The sixth chrome spinel layer is orthocumulate textured; it thickens locally up to 15 cm and presents a small adcumulate lens at the base. A coarser grained anorthositic gabbro of 4 m thickness is intercalated between the sixth and seventh chrome spinel bands. The latter bifurcates locally into two thin bands, and thickens up to 25 cm before pinching out over a few meters. An anorthositic gabbro 75 cm thick lies in the uppermost portion of cycle 4 which terminates with a sharp upper contact.

CYCLE 3 is about 9 m thick. Its lower contact is irregular and exhibits magmatic troughs filled by discontinuous layers. Thin chrome spinel seams overlain by pegmatitic patches are sparsely distributed in the lower portion. Three chrome spinel layers occur in the middle portion of the cycle. They all display fluid escape, and drop and sag structures. The lower adcumulate textured chrome spinel band pinches out locally and thickens up to 15 cm. It is overlain by a 1 m thick orthocumulate layer. The two upper spinel layers are disrupted orthocumulates and are separated by an olivine gabbro layer 90 cm thick. Cycle 3 is capped by a 0.8 m thick anorthositic gabbro layer.

CYCLE 2 is about 10 m thick. The upper 1.50-1.80 m is composed of anorthositic gabbro easily recognizable on the cliffs, and the remaining lower portion consists of chrome spinel bearing rocks. Drop and sag structured thin chrome spinel adcumulate seams occur in the three meters thick lower portion. Sulphides are scattered within orthocumulates and pegmatitic patches.

Three slumps overlying each other are observed in the middle portion of the cycle 2. The slumps consists of a mixture of deformed chrome spinel adcumulate, orthocumulate layers and cognate xenoliths. The matrix of the slumped material is orthocumulate textured and shows planar lamination which dips southerly. This is consistent with basin shaped layering of the intrusion and

indicates that slumping occurred southward and downward on the northern flank. Some sulphide blebs are polarity textured, but the top and bottom of this polarity is no longer oriented in the vertical direction. The lowermost slump is about 3 m in strike length and 1 m deep. It is capped by a continuous chrome spinel layer. The latter was clearly deposited after the first slump occurred. A discontinuous pegmatitic gabbro 1 meter thick is intercalated between slumps 1 and 2. The second slump is approximately 6 m long and 2 m deep. Its lower curved slide surface is particularly well defined by strongly disrupted adcumulate layers which are fragmented into angular blocks. The second slump is truncated and partly capped by the third slump which is approximately 4 m long and 0.60 m thick. The upper slump consists mainly of fine grained olivine-chrome spinel orthocumulate. The contact between the third slump and overlying anorthositic gabbro is sharp, and is the site of several chrome spinel bearing xenoliths.

CYCLE 1 is thickest and measures 14 m. The lower 10 m consists of chrome spinel gabbros, and is separated from the overlying anorthositic gabbro by a sharp contact which is locally faulted. The passage between unlayered lower zone and cycle 1 is gradational.

Thin chrome spinel seams in the basal portion of cycle 1 are overlain by drop and sag structured adcumulate layers. Thickness of the chrome spinel adcumulates ranges from a few mm to about 15 cm. Load casts and fluid escape structures are also observed. While the lower sags are a few cm across, the upper ones just beneath the anorthositic layer are up to 50 cm deep. The sides of the sag structures become steeper beneath the anorthositic gabbros. Pegmatitic gabbros underlie and overlie most of the sag structures. When followed laterally some sags pass into a thin chrome spinel layer. The sags exhibit various filling material: they may contain chrome spinel orthocumulate and/or strongly deformed adcumulate layers and cognate xenoliths. Sulphides are scattered within and outside of the sags, and some display polarity textured blebs.

Cognate xenoliths are abundant and prominent in cycle 1. They occur within and outside of the sag structures. Xenoliths are fine to medium grained and may contain chrome spinel. The chrome spinel-bearing xenoliths are all adcumulate textured and are probably the ultimate product of the drop and sag mechanism. The chromite free xenoliths are subangular and orthocumulate textured. Their size ranges from a few cm to 30-40 cm. At about 2.25 m from the base of the cycle three medium grained cognate xenoliths lying side by side are capped by a chrome spinel orthocumulate layer. But a few meters stratigraphically higher, a fine grained cognate xenolith has produced load cast structures in the underlying spinel layers.

V.3.C Mineral Chemistry

Compositions of silicates in adcumulate and orthocumulate rocks were analysed, and data are given in Tables 9 to 11. A minimum of five analyses were performed per silicate grain, and the results are averaged.

PLAGIOCLASE: two generations of plagioclase are distinguished, early and late. The former is characterised by its patchy zoning while the second is always normally zoned. Numerous plagioclase grains display a patchy core surrounded by a normally zoned margin (Photos 1 to 4). Patchy zoned crystals have higher An content, ranging between 85 and 70%. Normally zoned plagioclases have lower An content ranging from 70% to 30%.

OLIVINE exhibits various textural forms: equant, euhedral to subhedral, poikilitic, and interstitial. In most cases it occurs as large oikocrysts. The poikilitic olivine exhibits in general intergrowth textures with plagioclase which is often left as relicts. The chrome spinel inclusions in olivine may be surrounded by a thin plagioclase envelope (Photos 11, 12). The interstitial olivine may form upwardly elongated and branching skeletal crystals. Sulphide inclusions occur rarely in olivines.

Olivine presents significant compositional variations depending on the rock textures, presence of chrome spinel inclusions, olivine texture, and disruption of the host rock, as follows;

- a) In adcumulate rocks olivines are richer in Fo (about 76-81%) than those in orthocumulates (57 and 72%).
- b) Olivine that hosts chrome spinel inclusions has a higher Fo content (3-4%) than those which do not.

c) Poikilitic olivines which resorb plagioclases are richer in Fo (68 to 75%) than interstitial ones (58 to 69%).

d) Fo in olivine in disrupted rocks whether adcumulate or orthocumulate is lower in general than in undeformed rocks. For example olivine in the undisrupted spinel layers of the fourth cycle always have higher Fo than those in similar disrupted layers of the lower cycles.

AUGITE is the major intercumulus mineral. It forms large oikocrysts. In coarse grained to pegmatitic gabbros it forms elongated crystals that do not completely enclose plagioclase. It may contain chrome spinel and sulphide inclusions. Those containing chrome spinels are richer in Cr₂O₃. Polarity textured sulphides are capped by augite whose composition is enriched in FeO (Fig.10A).

ORTHOPYROXENE occurs as an accessory mineral displaying epitactic relations to olivine and augite. In the former it often shows symplectic intergrowth with plagioclase at the margin of the olivine in association with biotite and ilmenite, and tends to be richer in MgO (Fig.10 A). In the latter it tends to rim augite.

HORNBLLENDE always occurs in epitactic relation to augite, and its Fe content varies depending on that of the host augite (Fig.10A).

BIOTITE occurs in three textural forms in accessory amounts. It may be epitactic to olivine and augite, or interstitial, or may contain chrome spinel and sulphide inclusions. It presents a large range of chemical compositions depending on its textural form. Biotite occurring epitaxially with olivine is richer in MgO. When it is interstitial or epitaxial to augite it is enriched in FeO. A complete spectrum of compositions exists between these two extremes (Fig.10B).

CI-APATITE is often associated with biotite. It also forms prismatic crystals in the upper portion of the polarity textured sulphide blebs.

CHROME SPINEL forms rounded, euhedral to subhedral, sintered, and irregular crystals. It exhibits three textural forms: 1) inclusions within cumulus silicates, 2) inclusions in the overgrowths on cumulus minerals, and in intercumulus minerals, and 3) intercumulus grains.

Chrome spinel presents significant compositional variations depending upon host rock texture, host mineral, and location within the host mineral. These textural features tend to reflect the timing of crystallization and/or re-equilibration of the chrome spinel (Cogulu, 1988b).

ILMENITE is the principal oxide phase in pegmatitic gabbro and occurs as large, irregular skeletal crystals. In the spinel bearing gabbros ilmenite may in addition form exsolution lamellae within intercumulus chrome spinel grains.

SULPHIDES are represented by a troilite-hexagonal pyrrhotite-pentlandite-chalcopyrite-cubanite assemblage. The last two sulphides are dominant. In addition to the textural varieties mentioned in the lower zone, sulphides also exhibit polarity textured blebs in the cyclic zone.

VI ROCK CHEMISTRY

Seventy representative rock samples from different zones were analysed by XRF for major and trace elements. Rare-earth element concentrations were determined by INAA on thirteen samples. The data are given in Tables 12 to 21.

VI.1 MAJOR ELEMENTS

BASAL ZONE. Major oxides in drill hole 18 are plotted against depth (Figs 11, 12). Fine grained basal gabbro is significantly enriched in SiO₂ and K₂O. This reflects the more felsic and biotite-richer modal composition of the rock.

LOWER UNLAYERED ZONE. Rocks of sub-units A, B and C are relatively uniform in composition. But the sample from the middle portion of the Unit B shows an increase in SiO₂, CaO and Al₂O₃, and lowered MgO and Fe₂O₃. As mentioned above, this rock contains felsic materials displaying characteristic granophyric-micrographic textures. This is probably due to local contamination by sedimentary xenoliths which are sparsely distributed in the LUZ.

CYCLIC ZONE. Chrome-spinel bearing rock is poorer in SiO₂, Al₂O and K₂O, but richer in MgO, Fe₂O₃ and TiO₂. Conversely the anorthositic gabbros in the upper portion of the cycles are richer in SiO₂, Al₂O₃ and K₂O, but poorer in MgO, Fe₂O₃ and TiO₂.

AFM diagrams of rocks from different zones are shown in Figs.13 A, B and C. Basal zone gabbros are richest in $K_2O + Na_2O$. Those of the lower unlayered zone have a limited range of variation and cluster together except for the contaminated gabbro of sub-unit B which has a distinctive composition. The rocks of the cyclic zone exhibit a large range of variation. SiO_2 versus MgO and Al_2O_3 versus CaO variations of rocks in the cyclic zone are plotted in Fig.14, A and B. Rocks of the cyclic zone become progressively poorer in MgO, but richer in Al_2O_3 , CaO, and FeO* from chrome spinel adcumulates to anorthositic gabbros. Adcumulates are poorest in alkalis while anorthositic gabbro has the highest alkali content. These data demonstrate that gabbros in the cyclic units are products of differentiation by fractional crystallization.

VI.2 TRACE ELEMENTS

Trace elements partitioned into cumulus phases are compatible, and those carried in the intercumulus phases tend to be incompatible. Trace element abundances vary as the parent magma evolves or new magma batches are introduced. Rb, Sr and Zr variations versus depth are plotted in Fig.15. Rb is an incompatible element whose abundance is controlled by the amount of intercumulus material. Basal gabbro is enriched in Rb as well as in K; this would reflect the abundance of the trapped intercumulus liquid and the contamination by partial melting products of the country rocks. Rb is quite uniform in the lower unlayered zone, but shows large fluctuations between chrome spinel bearing rocks and anorthositic gabbros in the cyclic zone. The latter are always richer in Rb.

Sr is a compatible element which reflects plagioclase variations with depth. Its abundance correlates well with Ca. The lower zone shows a small range of Sr. The anorthositic gabbros of the cyclic units are significantly enriched in Sr, reflecting the plagioclase abundance in these rocks.

Zr abundances in the LUZ are erratic, and higher than in the Cyclic zone. Gabbros in the lower portions of the cyclic units are depleted in Zr while anorthositic gabbros are relatively enriched.

VI.3 RARE-EARTH ELEMENTS (REE)

Whole-rock rare earth abundances in different zones are detailed in Tables 19 to 21, and summarized in Table 22. The diagrams of Fig.16 show chondrite normalized REE patterns for each of the three zones. A comparative summary diagram of REE patterns in the three zones is given in Fig.17.

Gabbros of the Crystal Lake intrusion are depleted in the heavy REE (HREE) compared to the light REE (LREE). LREE/HREE ratios differ from zone to zone.

Basal zone gabbros have the highest total REE values, and the La/Yb ratios range from 6.86 to 12.60. There is no Eu anomaly in the basal zone. Gabbros of the LUZ have HREE values similar to those of the basal zone, but their LREE values are somewhat lower, resulting in lower La/Yb ratios. In general there are no Eu anomalies in the LUZ.

REEs in gabbros of the cyclic units differ greatly from those of the lower zones. The total REE content of cyclic gabbros is less than one half that of the basal zone gabbros. Furthermore, chondrite normalized REE patterns in the cyclic zone show shallower slopes and lower La/Yb ratios (6.28 to 7.81). Finally, cyclic zone gabbros are characterized by positive Eu anomalies.

VII DISCUSSION AND INTERPRETATION

Recent studies carried out on the Duluth Complex have demonstrated the importance of country rock contamination. However there is disagreement on the timing of contamination, and on the role of partial melting and country rock assimilation. Sulphur and oxygen isotope studies of the Dunka Road Cu-Ni deposit (Rao and Ripley, 1983; Ripley, 1986) reveal that assimilation of country rock was restricted to areas near country rock xenoliths. On the basis of silicate and sulphide mineralogy of the Partridge River troctolite, Tyson and Chang (1984) concluded that a hydrous sulphur-bearing fluid which was derived from the country rocks was the main contaminating agent. It also transported copper, iron and alkalis into the magma early in the crystallization. Mainwaring and Watkinson (1981) too, suggested early country rock contamination and proposed that the compositional changes of chrome spinels in the Crystal Lake intrusion "may

have resulted from reaction of early cumulus spinels with gabbroic liquids which underwent contamination by assimilation of aluminous country rocks". But according to Grant and Molling (1981), Chalokwu (1985), and Chalokwu and Norman (1987) the compositional changes of the mafic minerals in the Partridge River troctolite are not related to contamination of the magma; they are the result of re-equilibration of cumulus minerals with iron rich intercumulus liquid.

There are significant petrological and chemical differences between various zones of the Crystal Lake intrusion. The basal zone contains fine grained orthocumulate gabbros and felsic materials which are products of partial melting of the country rocks. As a result, the modal proportions of orthopyroxene, biotite and sulphides are increased. Olivine has not been observed in this zone. Bulk rock chemistry indicates that the basal zone is enriched in SiO_2 , K_2O and Rb. Crystallization of the orthopyroxene instead of olivine may be explained by the addition of SiO_2 from the country rock before the nucleation of the olivine. The high biotite abundance may also be explained by H_2O and K addition from the devolatilization of the sedimentary contact rocks. As documented by Eckstrand and Cogulu (1986) and Cogulu (1988a) sulphur derived from the Rove Formation was incorporated into the magma and resulted in formation of the sulphides.

The orthocumulates of the LUZ do not display any significant variations in bulk composition except in the areas near sedimentary xenoliths. Mafic minerals exhibit cryptic variation patterns which are not related to contamination. The olivine is mostly intercumulus except at the base of sub-unit B. The compositional differences shown by olivine are due to new influx of magma and the re-equilibration with iron rich trapped intercumulus liquid. The SiO_2 enrichment of gabbros in the middle portion of sub-unit B may be explained as a local contamination by partial melting of sedimentary xenoliths.

The cyclic zone differs greatly in mineral and rock chemistries from the other zones. These rocks are more differentiated, and have a larger range of whole-rock and modal compositions. Bulk compositions of the rocks are related to differentiation of the magma, and there is no evidence of country rock contamination. Adcumulate rocks are often associated with chrome spinel mineralization and represent Mg rich gabbros while anorthositic gabbros are the most differentiated and enriched in alkalis and iron. All intermediates between these two extremes exist within the cyclic units.

Another characteristic feature of the cyclic zone is the soft sediment-like deformation observed in chrome spinel bearing rocks. The drop and sag structures described in these rocks may be formed in different ways. Some sags, especially those underlain by pegmatites, may be the result of sagging and thickening. Others may be primarily magmatic troughs, created and filled by the action of convection currents as they formed; this would be the case for the sags containing folded and disrupted adcumulate bands.

The fine grained cognate xenoliths are considered to have been brought in a solid state from the marginal zone of the intrusion by magmatic currents. Their transport occurred at an early stage of magma crystallization.

As crystallization progressed, soft sediment type deformation, magmatic current activities, and upward migration of the pegmatitic material occurred together. Presence of slumps indicates that the initial deposition surface was an inward slope along which turbidite-like mass transport occurred. Presence of strongly disrupted chrome spinel adcumulates and angular cognate xenoliths at the base of slumps may indicate that the contact between adcumulate and underlying orthocumulate played the role of a glide surface. Sharp contacts between anorthositic gabbros and underlying chrome spinel bearing rocks of cycles 1 and 2 may correspond to erosional surfaces as indicated by the presence of cognate xenoliths.

No rocks in the Duluth Complex, comparable to the cyclic zone (enriched in chromite and PGE) of the Crystal Lake intrusion have yet been documented.

VIII CONCLUSIONS

The western portion of the Crystal Lake intrusion comprises four main zones which differ from each other in mineral and rock chemistries and textures. The basal zone representing the chilled margin of the intrusion is contaminated by underlying sedimentary Rove Formation. Contamination was accomplished by two mechanisms: dehydration and partial melting. Sulphur, alkalis, water, silica and chlorine are the main contaminants.

The lower unlayered zone which hosts the major portion of the sulphide mineralization is composed of weakly differentiated orthocumulate rocks. The major element contamination is restricted to areas surrounding sedimentary xenoliths. Three sub-units, A, B and C, each probably corresponding to fresh magma introduction, exhibit characteristic cryptic variation patterns of mafic minerals.

The cyclic zone, composed of four superposed magmatic cycles, contains the most differentiated rocks of the intrusion. The cycles correspond to repeated magma influx. The processes of double-diffusive fractional crystallization and infiltration metasomatism as described by Irvine (1980) may provide explanations for many of the petrologic features. Soft sediment-type deformation occurred before the re-equilibration of the olivine with intercumulus liquid. The cyclic units do not display any evidence of contamination by country rocks.

The contents of REE and the LREE/HREE ratios decrease upward in the intrusion. The cyclic units are distinctly more impoverished in REE compared to lower zones, and display positive Eu anomalies in their chondrite normalized patterns. Eu anomalies decrease with increasing total REE content.

ACKNOWLEDGMENTS

Support of the Geological Survey of Canada is gratefully acknowledged. The author is particularly grateful to O.R.Eckstrand for his helpful comments, and to J.M.Duke, and R.F.J.Scoates for their constructive criticism. Thanks are also extended to D.C.Harris, G.J.Pringle, M.Bonardi, G.Lecheminant, and A.G.Plant for their assistance with microprobe analyses.

The author also extends thanks to J.P.McGoran, Fleck Resources Ltd., and to Boliden Canada Ltd. for access to the property and drill core.

This work was funded in part by grant A0590 from the Natural Sciences And Engineering Research Council of Canada.

REFERENCES

- Arth, J.G., 1976, Behavior of trace elements during magmatic processes. A summary of theoretical models and their applications; *J. Res. U.S. Geol. Surv.* v.4, p.41-47.
- Chalokwu, C.I. and Grant, N.K. 1983, The importance of trapped liquid abundances to the reequilibration of primary mineral compositions in the Partridge River troctolite, Duluth Complex, Minnesota, *Geol.Soc.Am. Abstr. with programs* v.15. p.541.
- Chalokwu, C.I., 1985, A geochemical, petrological and compositional study of the Partridge River intrusion, Duluth Complex, Minnesota. (Ph.D.thesis) Oxford, Ohio, Miami University, 232 p.
- Chalokwu, C.I., 1987, Reequilibration of olivine with trapped liquid in the Duluth Complex, Minnesota; *Geology*, v.15, p.71-74.
- Chase, C.G., and Gilmer, T.H., 1973, Precambrian plate tectonics: The midcontinent gravity high. *Earth Planet. Sci. Lett.*, v.21, p.70-78.
- Cogulu, E.H., 1984, Magmatic cycles in the Crystal Lake gabbros, Thunder Bay, Ontario. *Geol. Ass. Can. Ann. meeting, Abstr. with programs*, p.53.
- Cogulu, E.H., 1985, Platinum group elements and chromian spinel variations in the Crystal Lake gabbros, Thunder Bay, Ontario. *Fourth Int.Platinum Symp. Abstr. Can. Mineral.* v.23, p.299-300.
- Cogulu, E.H., 1988a Mineralogy and Chemical variations of sulphides in the Great Lakes Nickel deposit, Thunder Bay, Ontario. Report submitted to Geological Survey of Canada, Ottawa.
- Cogulu, E.H. 1988b, Factors controlling postcumulus compositional changes of chrome-spinels in the Crystal Lake intrusion, Thunder Bay, Ontario. Report submitted to Geological Survey of Canada, Ottawa.
- Geul, J.J.C., 1970, Devon and Pardee Townships and the Stuart Location; *Ont. Dep. Mines, Geol. report* 87, 52 p.
- Grant, N.K., and Molling, P.A., 1981, A strontium isotope and trace element profile through the Partridge River troctolite, Duluth Complex, Minnesota; *Contr. Miner. Petrology.* v.77, p.296-305.
- Hanson, G.N., 1980, Rare Earth elements in petrogenetic studies of igneous systems; *Ann. Rev. Earth Planet. Sci.*, v.8, p.371-406.
- Irvine, T.N., 1980, Magmatic infiltration metasomatism, double-diffusive fractional crystallization, and adcumulus growth in the Muskox intrusion and other layered intrusions, in Hargraves, R.B., ed., *Physics of magmatic processes*: Princeton, New Jersey; p.325-383.
- Irvine, T.N., 1982, Terminology for layered intrusions; *J. Petrol.*, v.23, p.127-162.
- Macrae, N.D., and Reeve, E.J., 1968, Differentiation sequence of the Great Lakes Nickel intrusion; *Abstr. 14th Ann. Meeting Inst. Lake Sup. Geol.*, Wisconsin State University.
- Mainwaring, P.R., and Watkinson, D.H., 1981, Origin of chromian spinel in the Crystal lake intrusion, Pardee Township, Ontario. *Ont. Geol. Surv. Misc. papers*, v.98, p.180-186.

Rao,B.V., and Ripley,E.M.,1983, Petrochemical studies of the Dunka Road Cu-Ni deposit, Duluth Complex, Minnesota. *Econ.Geol.* v.78, p.1222-1238.

Reeves,E.J., 1969, Petrology and mineralogy of a gabbroic intrusion in Pardee Township near Port Arthur, Ontario; Unpublished M.Sc thesis, University of Wisconsin.

Ripley,E.M., 1981, Sulfur isotopic studies of the Dunka Road Cu-Ni deposit, Duluth Complex, Minnesota; *Econ. Geol.* v.76, p.610-620.

Ripley,E.M., 1986, Application of stable isotopic studies to problems of magmatic sulphide ore genesis with special reference to the Duluth Complex, Minnesota,in Friedrich, G.H., ed., *Geology and metallogeny of copper deposits*. Springer-Verlag.

Scoates,R.F.J.,1983, A preliminary stratigraphic examination of the ultramafic zone of the Bird River sill, Manitoba; Dept. Ener. Mines, Report of Field Activ., p.70-83.

Scoates,R.F.J., Williamson,B.L., and Duke,J.M., 1986, Igneous layering in the ultramafic series, Bird River sill, in *Layered intrusion of southeastern Manitoba and northwestern Ontario; Field trip guidebook*, Geol. Assoc. Canada, Ann. meeting, Ottawa.

Seifert,K.E., and Brunfelt,A.O., 1982, REE composition of Duluth gabbro rocks, *Trans. Am. Geophys. Union*, v.63, p.615.

Seifert,K.E.,1984, Trace element geochemistry of some Lake Superior Keweenawan basic layered intrusions; *Abstr. 13th Annual Inst. Lake Sup. Geol.*, Wausau, Wisconsin.

Silver,L.T., and Green,J.C., 1972, Time constants for Keweenawan igneous activity; *Geol. Soc. Amer. Abstr. with programs*, v.4, p.665-666.

Sims,P.K., Card,K.D., and Lumbers,S.B., 1981, Evolution of early Proterozoic basins of the Great Lakes region; in *Proterozoic basins of Canada*, F.H.A.Campbell ed., *Geol. Surv. Canada paper* 81-10, p.379-397.

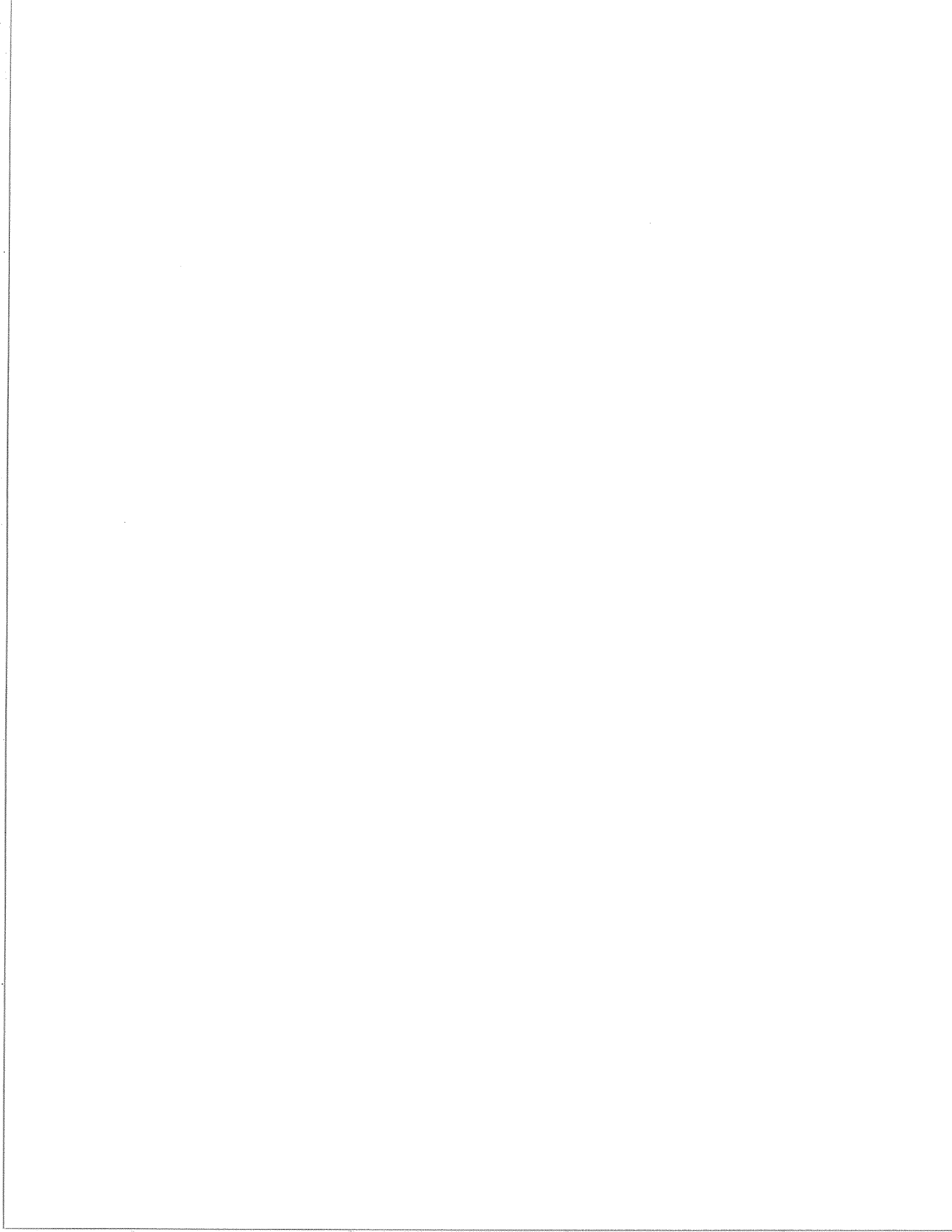
Stewart,A.D., 1963, On certain slump structures in the Torridonian sandstones of Applecross; *Geol.Mag.* v.100, pp.205-218.

Tyson,R.M., 1979, The mineralogy and petrology of the Partridge River troctolite in the Babbitt-Hoyt Lakes region of the Duluth Complex, Minnesota. (Ph.D.thesis), Miami University.

Tyson,R.M., and Chang,L.L.Y., 1984, The petrology and sulfide mineralization of the Partridge River troctolite, Duluth Complex, Minnesota. *Can. Mineral.* v.22, p.23-38.

Weiblen,P.W., 1982, Keweenawan intrusive igneous rocks; *Geol. Soc. Am. Memoir* 156, p.57-82.

Weiblen,P.W., and Morey,G.B., 1980, A summary of the stratigraphy, petrology and structure of the Duluth Complex, *Am. J. Sci.*, v.280A, p.88-133.



FIGURES

FIG.1. Map of the Mid-Continent Gravity High showing location of the Crystal Lake Gabbro.

FIG.2. Geological map of the Crystal Lake area (modified after Geul, 1970). AA' and BB' indicate the locations of the longitudinal and cross sections of Fig.5. The star indicates the site of surface sampling.

FIG.3. Lithologic units and their ages in the Crystal Lake area.

FIG.4. Stratigraphic column of the Crystal Lake Intrusion at the western end (revised after Geul, 1970).

FIG.5. Longitudinal and cross sections of the western end of the Crystal Lake intrusion (modified after Geul, 1970). Star indicates the site of surface sampling. Scale in metres.

FIG.6. Ca-Mg-Fe diagrams of augites and biotites in the Basal Zone. A) augites; B) biotites; crosses = biotites epitaxial to augite; rectangles = biotites associated with felsic material. (Atomic proportions).

FIG.7. Compositional variations of olivine and augite with stratigraphic height in the Lower Unlayered Zone.

FIG.8. Compositional variations of augites, showing effects of sulphides and rock types: Ca-Mg-Fe diagram, atomic proportions. A) Filled rectangles = augite with eutectoid-like sulphide inclusions; crosses = augite without sulphide inclusions; B) Filled rectangles = augites in pegmatitic gabbro; crosses = augites in cognate xenoliths..

FIG.9. Stratigraphic column of the Cyclic Zone. Thicknesses of the chrome spinel layers and seams are slightly exaggerated.

FIG.10. Ca-Mg-Fe diagrams of intercumulus minerals in the Cyclic Zone; atomic proportions. A) Filled rectangles = augites with sulphide inclusions; crosses = augites without sulphide inclusions; circles = hornblendes; X's = orthopyroxenes. B) Open rectangles = biotites in chrome spinel adcumulate layer; X's = biotites epitaxial to orthopyroxenes; filled rectangles = biotites epitaxial to augites or interstitial.

FIG.11. Variations in the concentrations of SiO_2 , CaO , Al_2O_3 , Na_2O , and K_2O with stratigraphic height in the Lower and Cyclic Zones.

FIG.12. Variations in the concentrations of MgO , Fe_2O_3 , and TiO_2 with stratigraphic height in the Lower and Cyclic Zones.

FIG.13. AFM diagrams for gabbros of the different zones of the Crystal Lake Intrusion. A) Basal gabbros; B) Lower Unlayered Zone; filled rectangles = contaminated gabbro in Unit B; crosses = fine to medium grained gabbros; open rectangles = cognate xenoliths in Unit C; C) Cyclic Zone; open circles = anorthositic gabbros; open rectangles = chrome spinel free orthocumulates; crosses = chrome spinel orthocumulate; filled rectangles = chrome spinel adcumulates; X's = chrome spinel bearing adcumulate xenoliths. ($\text{NA} + \text{K}_2 = \text{Na}_2\text{O} + \text{K}_2\text{O}$).

FIG.14. SiO_2 vs MgO and Al_2O_3 vs CaO in the Cyclic Zone. Symbols are the same as in Fig.13c.

FIG.15. Variations in the concentrations of Rb, Sr, and Zr with stratigraphic height in the Lower and Cyclic Zones.

FIG.16. Chondrite normalized REE profiles: A) Basal Zone; B) Lower Unlayered Zone; C) Cyclic Zone.

FIG.17. Comparison of chondrite normalized REE profiles: stippled = Basal Zone; crosses = Lower Unlayered Zone; outlined white = Cyclic Zone.

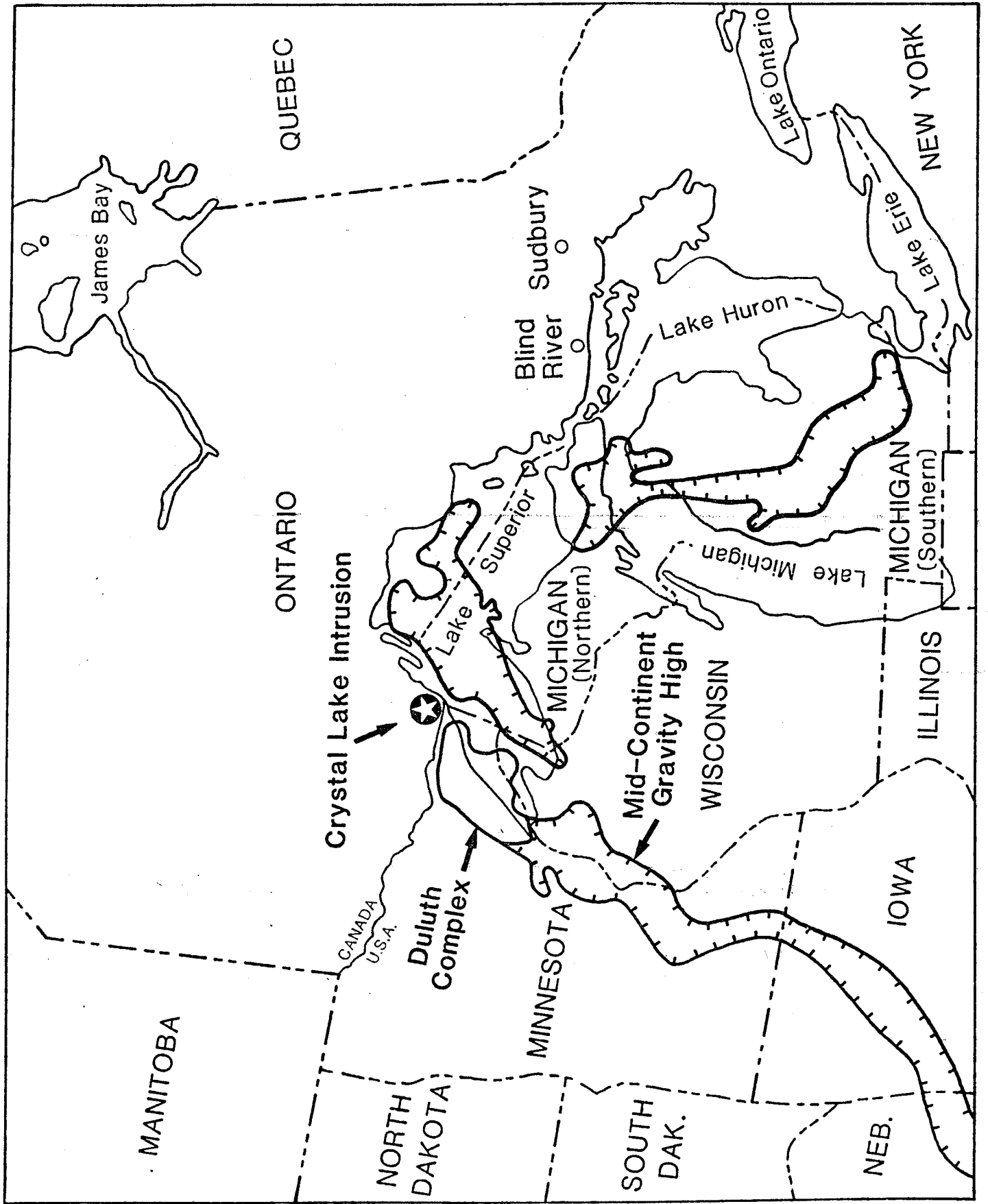
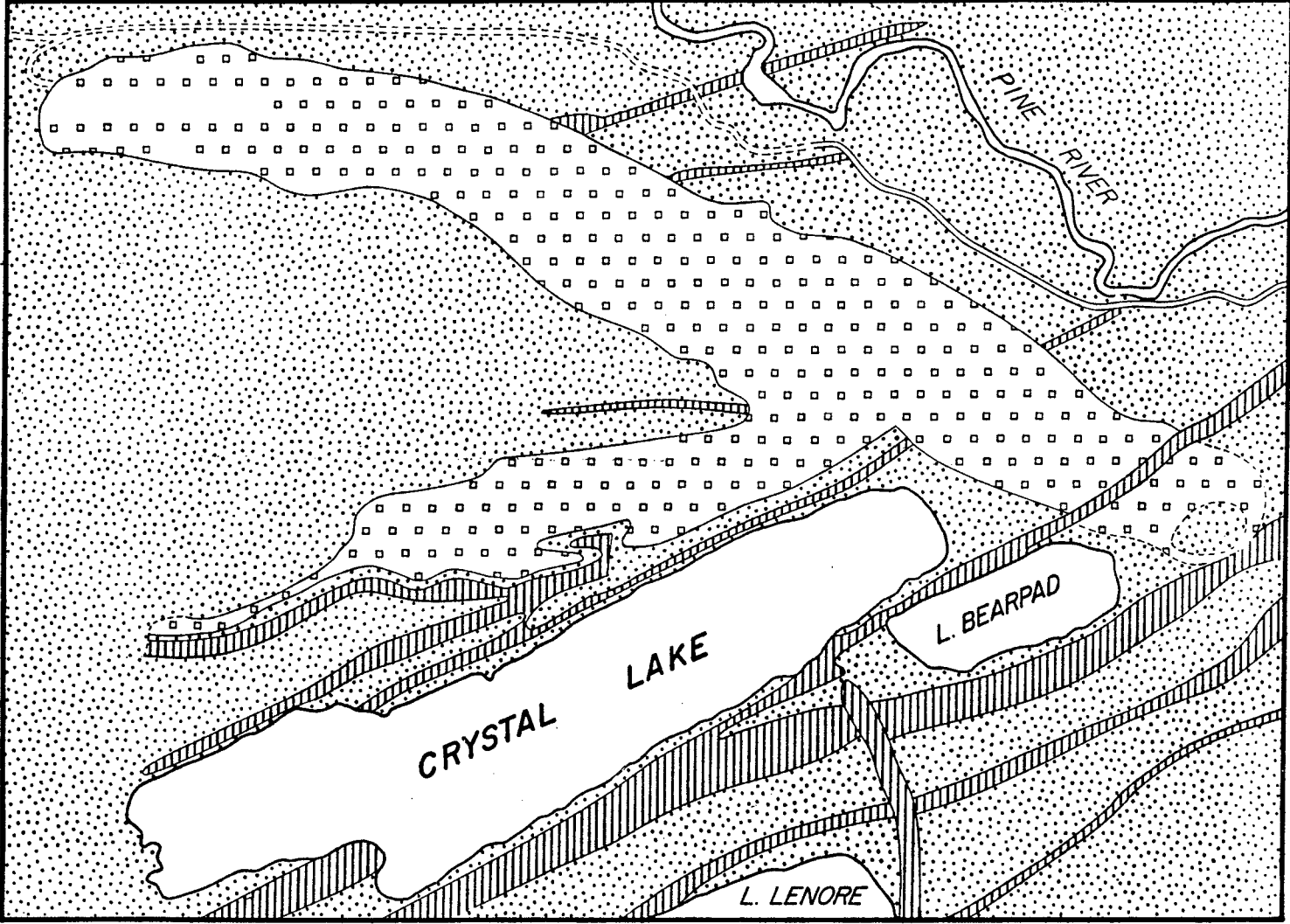
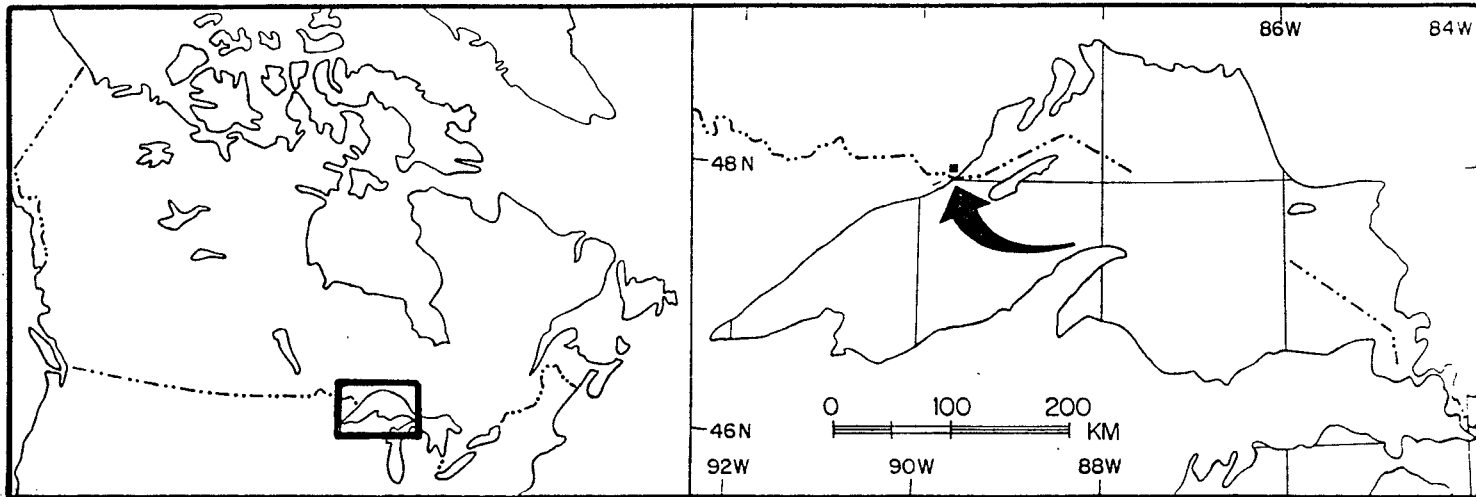


Fig. 1





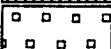
-  SEDIMENTARY ROCKS (ROVE FORMATION) AND GLACIAL DEPOSITS
-  PIGEON RIVER DIABASE DYKES
-  CRYSTAL LAKE GABBROIC INTRUSION

Fig. 2



LITHOLOGIC UNITS

Ages in 10 ⁶ years		QUATERNARY		GLACIAL DRIFT
UPPER PRECAMBRIAN		MIDDLE PROTEROZOIC	NORMAL	KEWEENAWAN LATE MAFIC AND FELSIC INTRUSIONS Diabase, Granophyre
				1100 CRYSTAL LAKE INTRUSION (RELATED TO DULUTH COMPLEX) Olivine Gabbro, Troctolite, Anorthositic Gabbro, Pegmatitic Gabbro
LOWER PROTEROZOIC		REV.	1200	PIGEON RIVER INTRUSIONS Olivine Diabase
				EARLY MAFIC INTRUSIONS: LOGAN SILLS Diabase, Tholeiite (Sill, Dyke)
1900-2000				ANIMIKIE ROVE FORMATION Argillite, Shale, Greywacke

Fig. 3

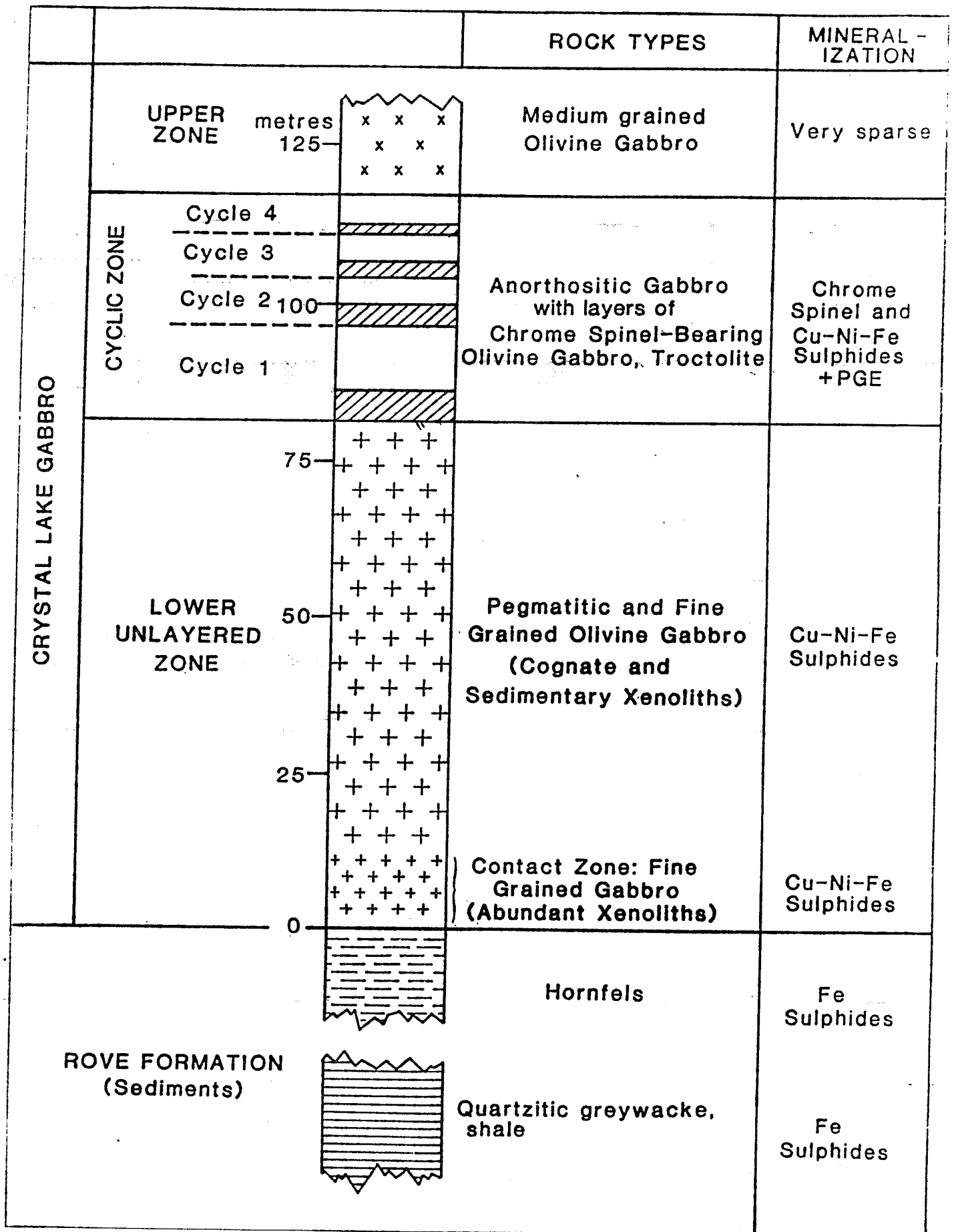


Fig. 4

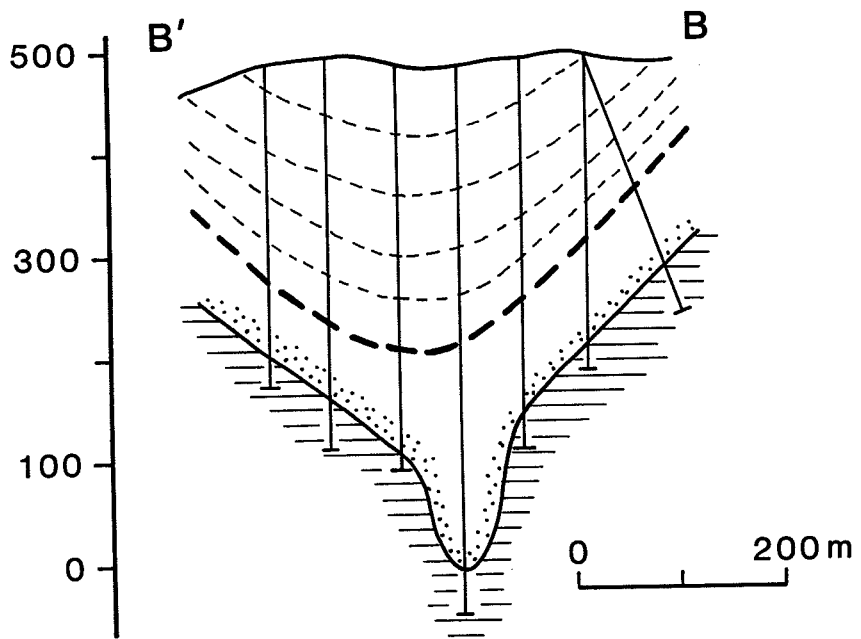
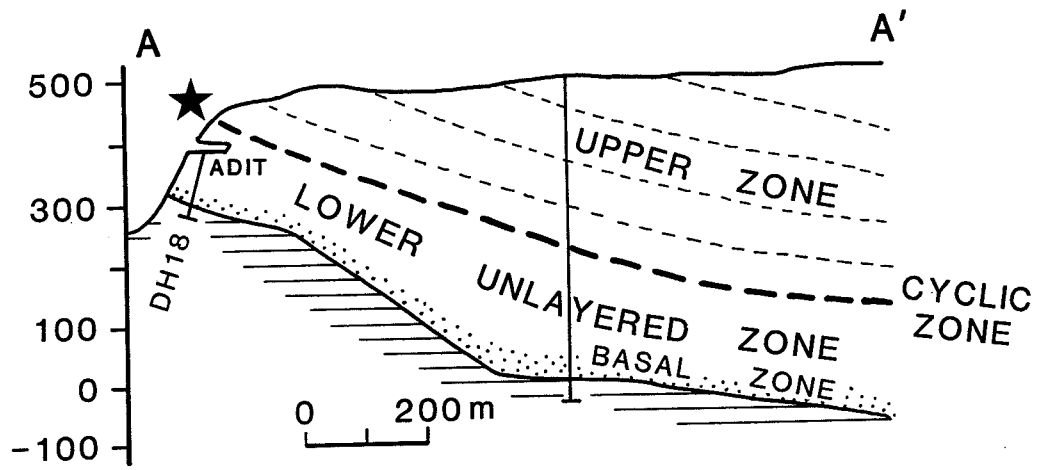


Fig. 5

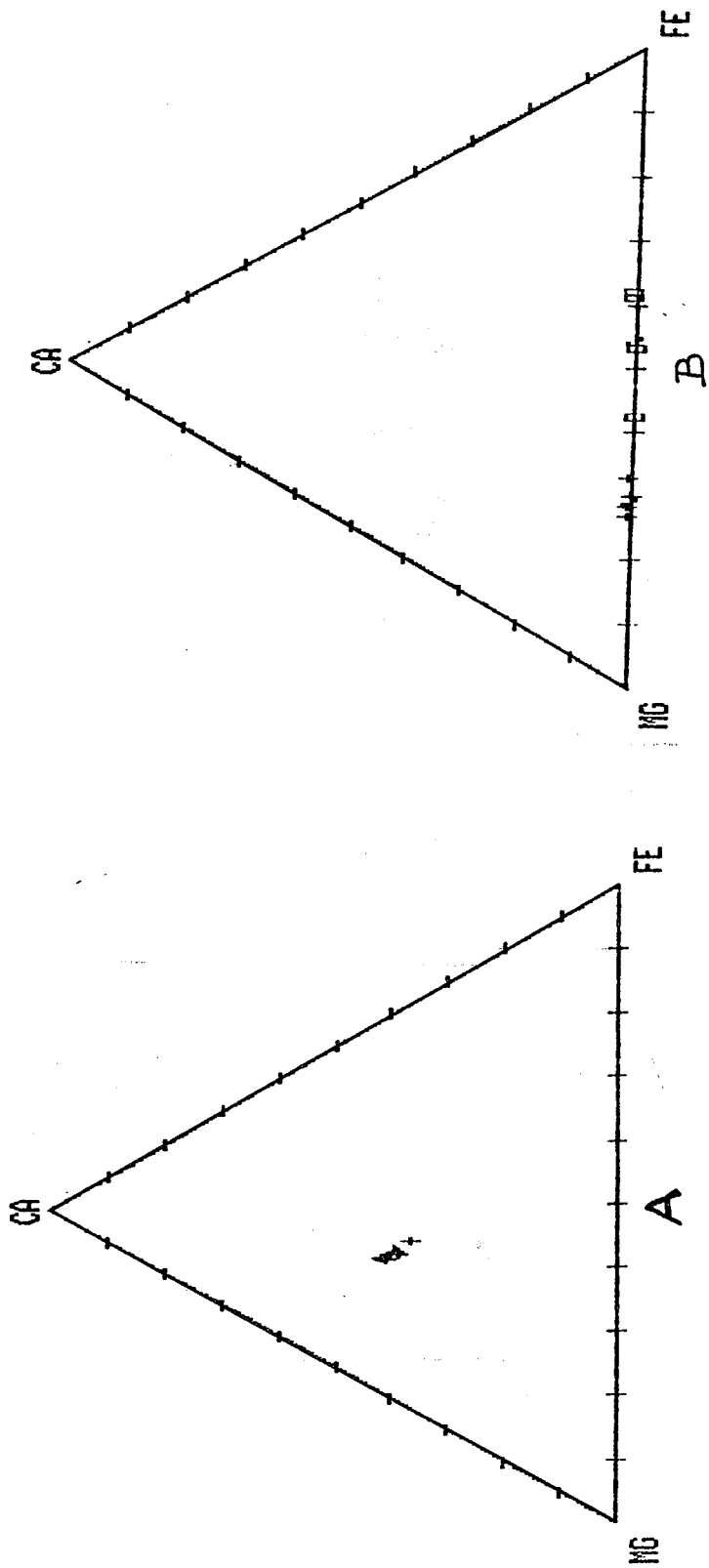


Fig. 6

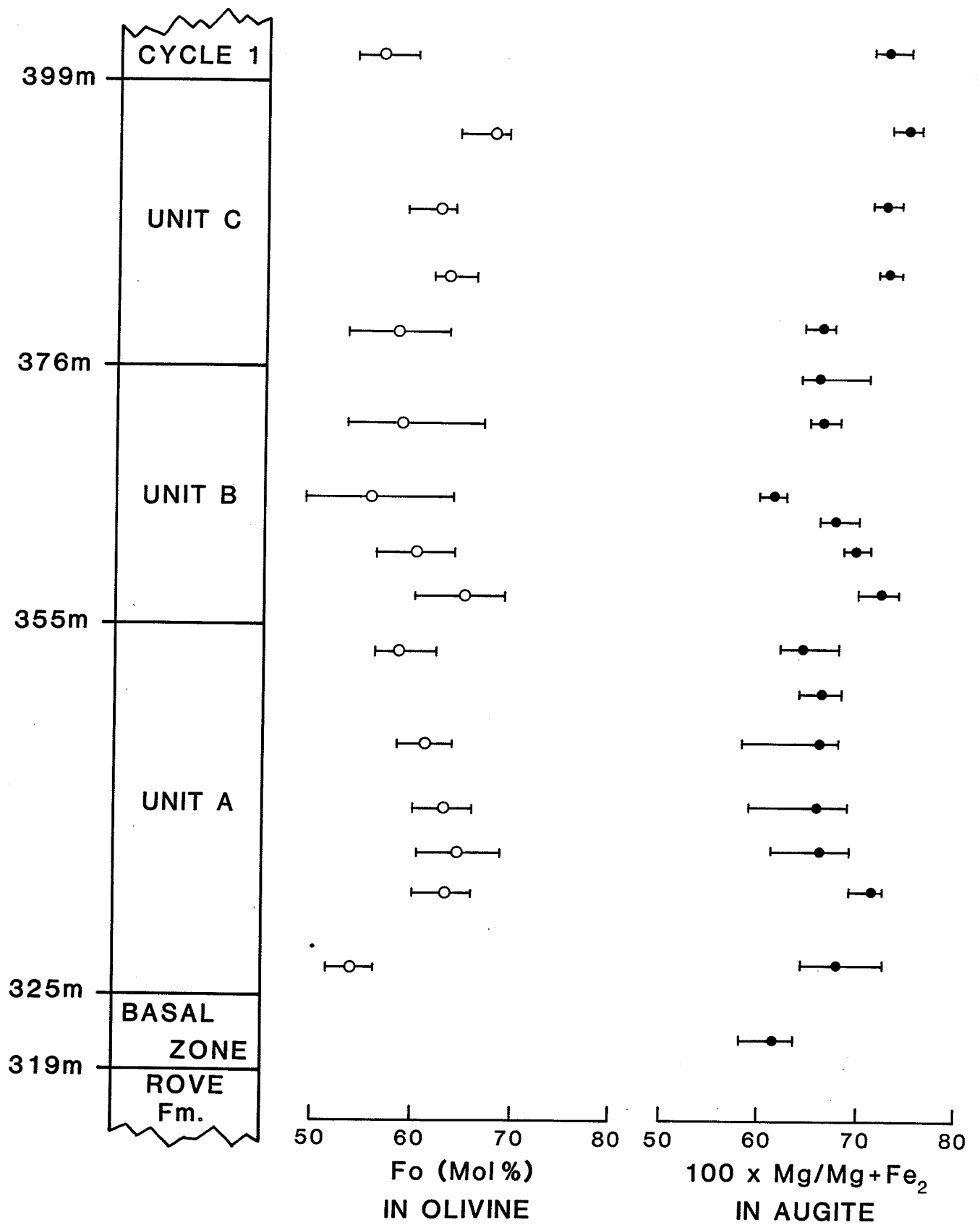


Fig. 7

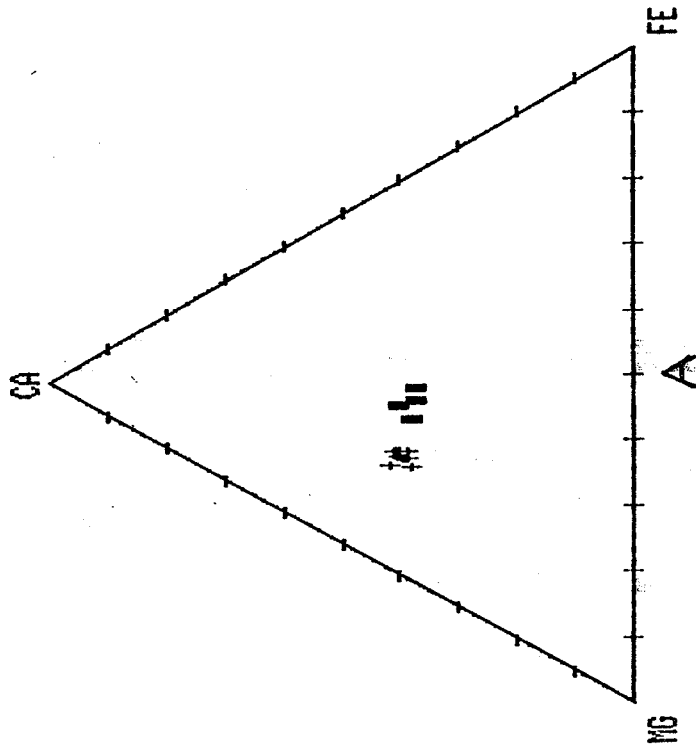
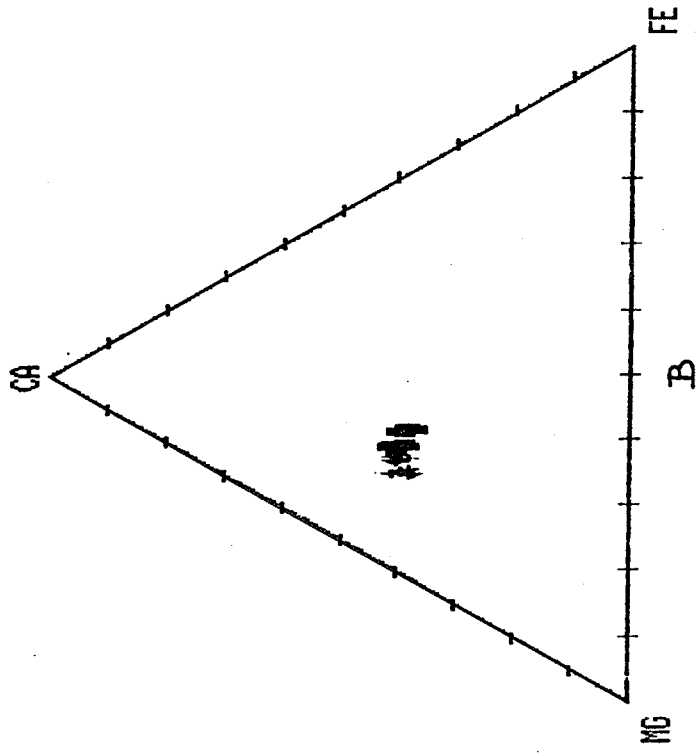


Fig. 8

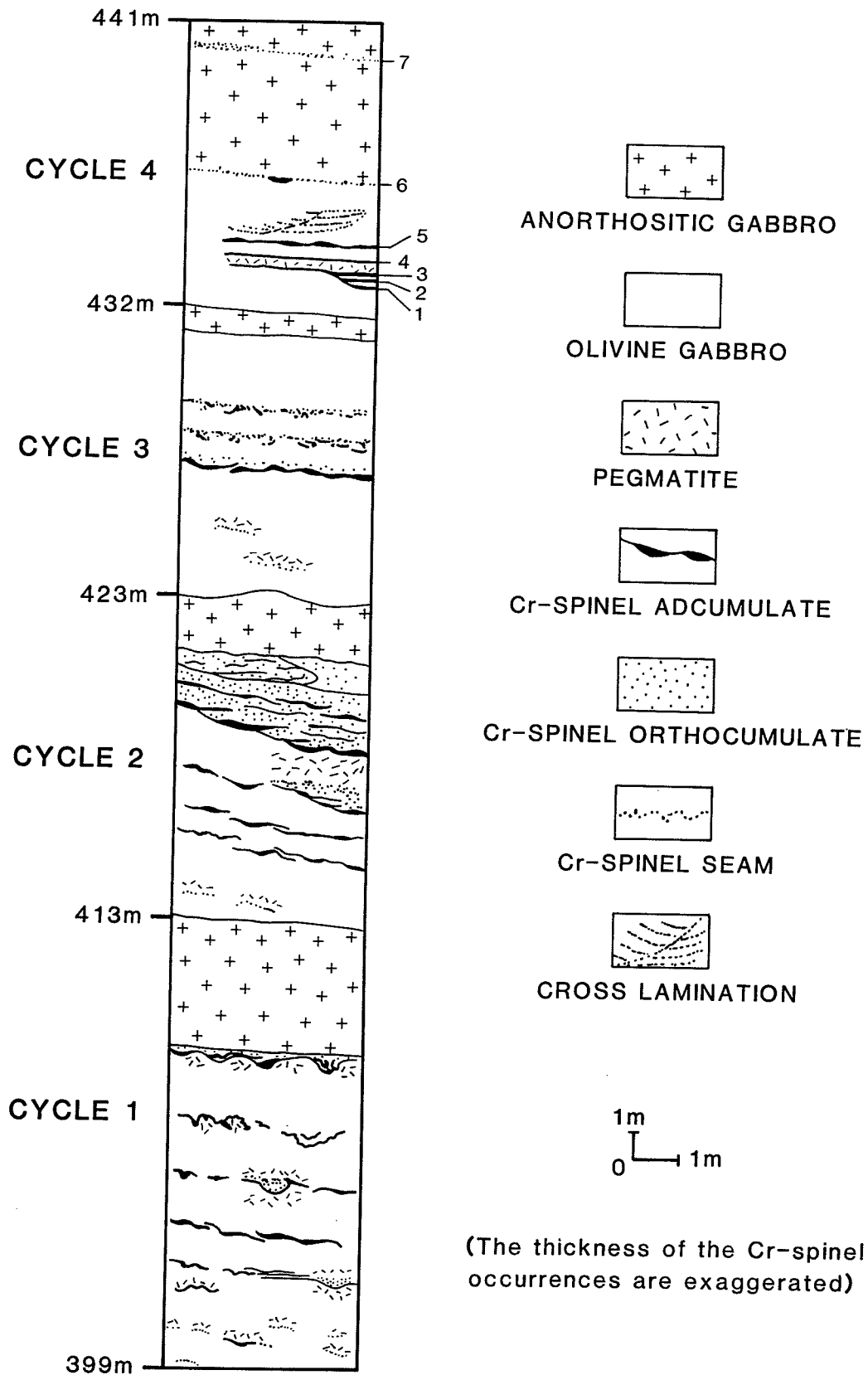


Fig. 9

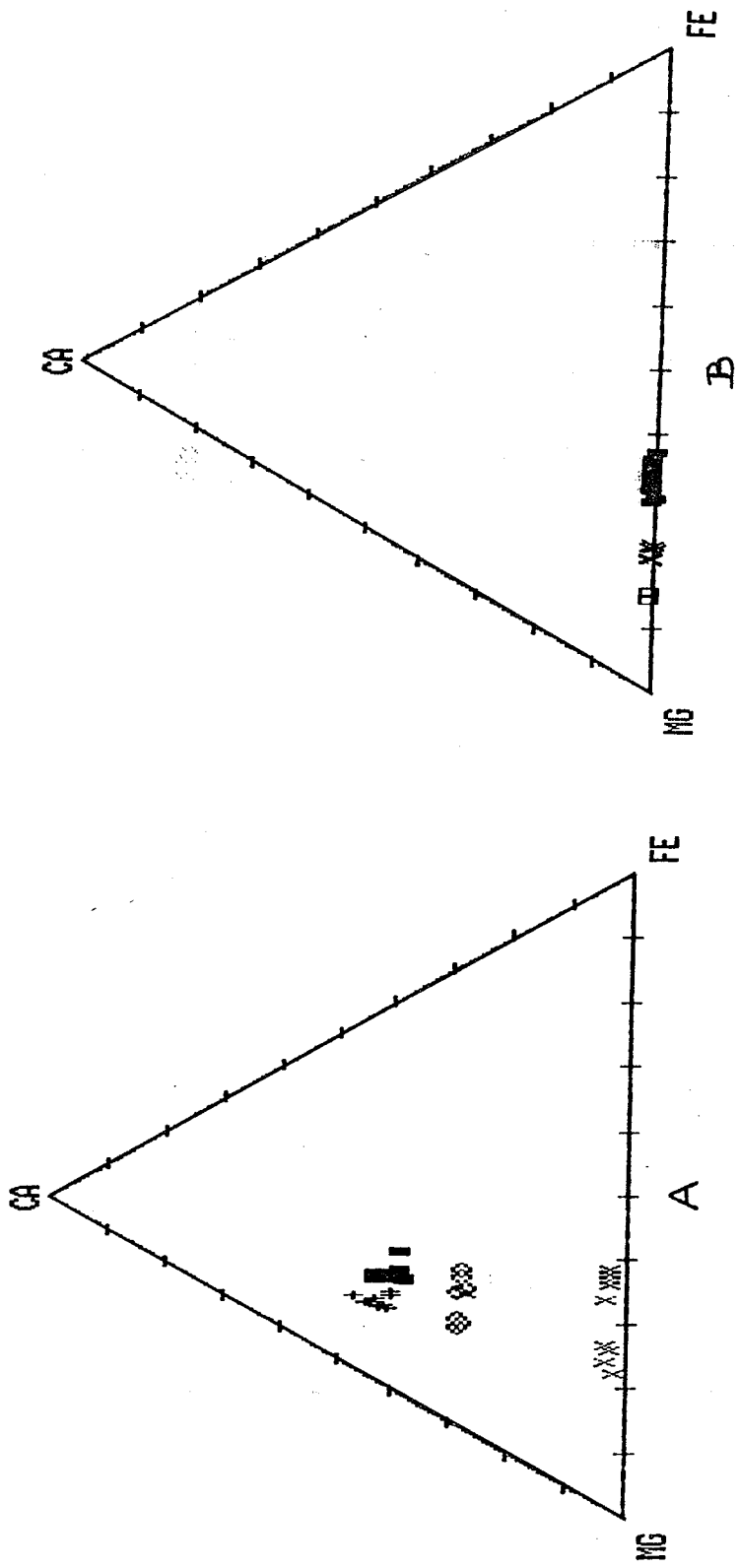


Fig. 10

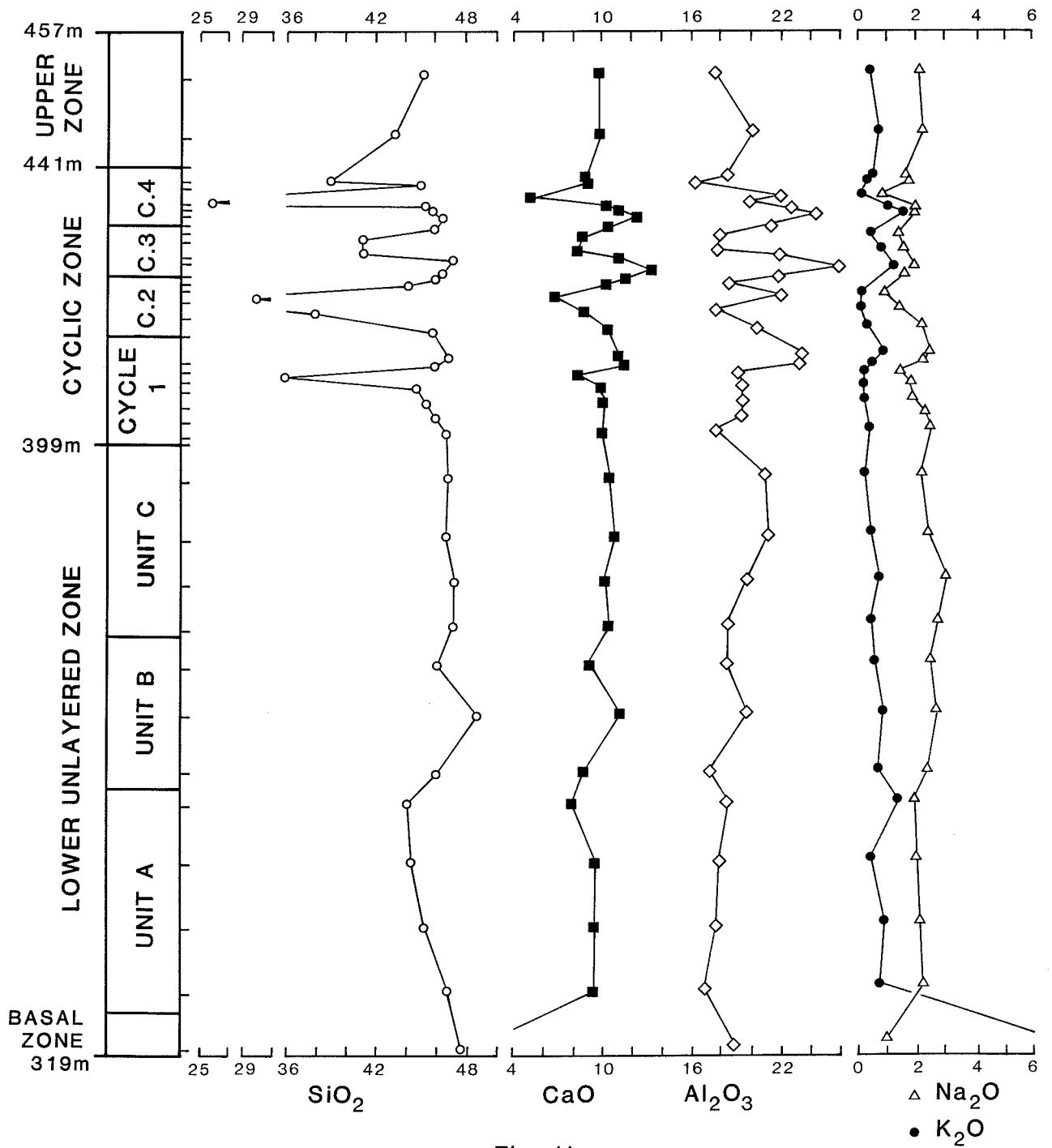


Fig. 11

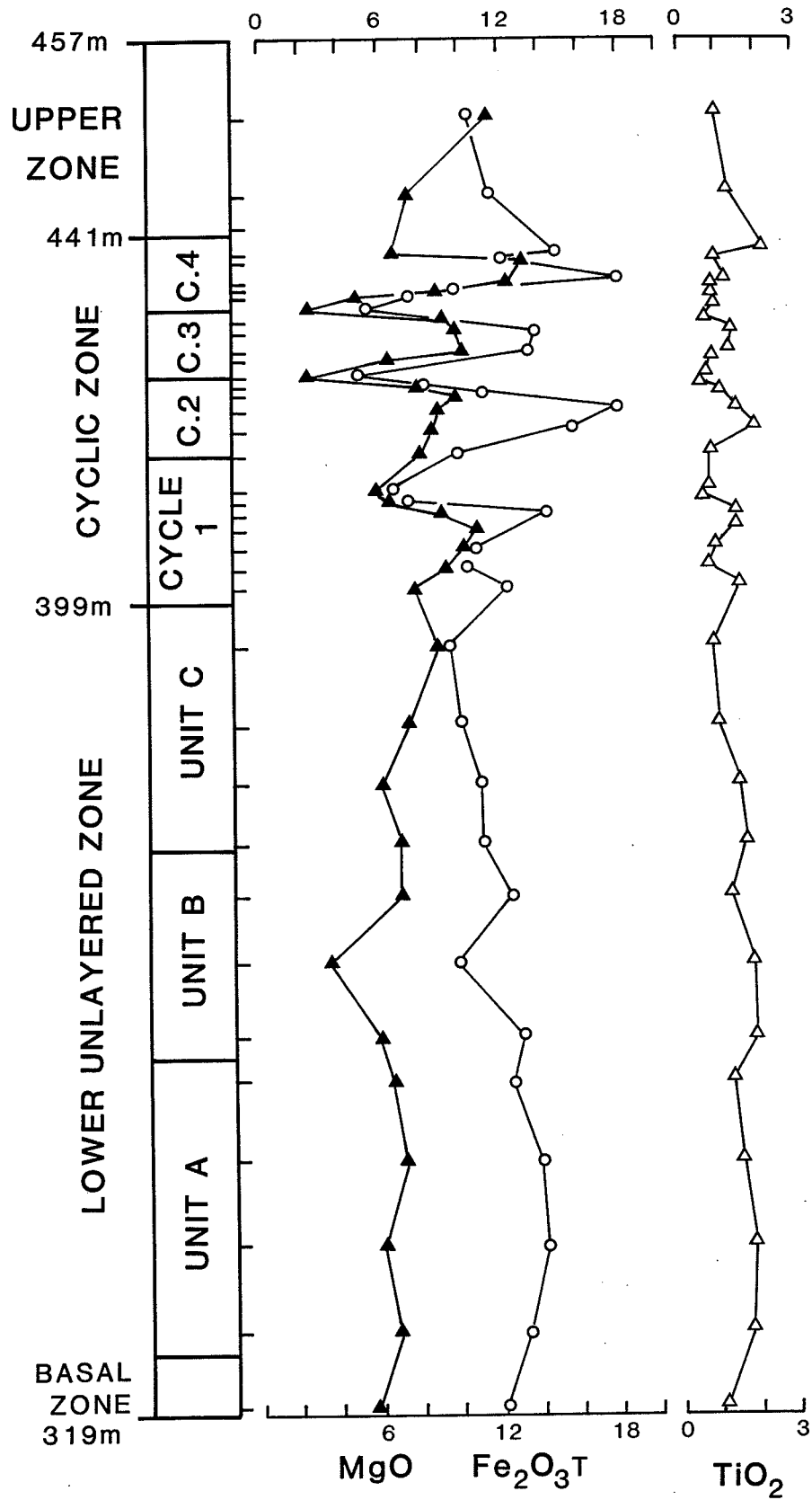


Fig. 12

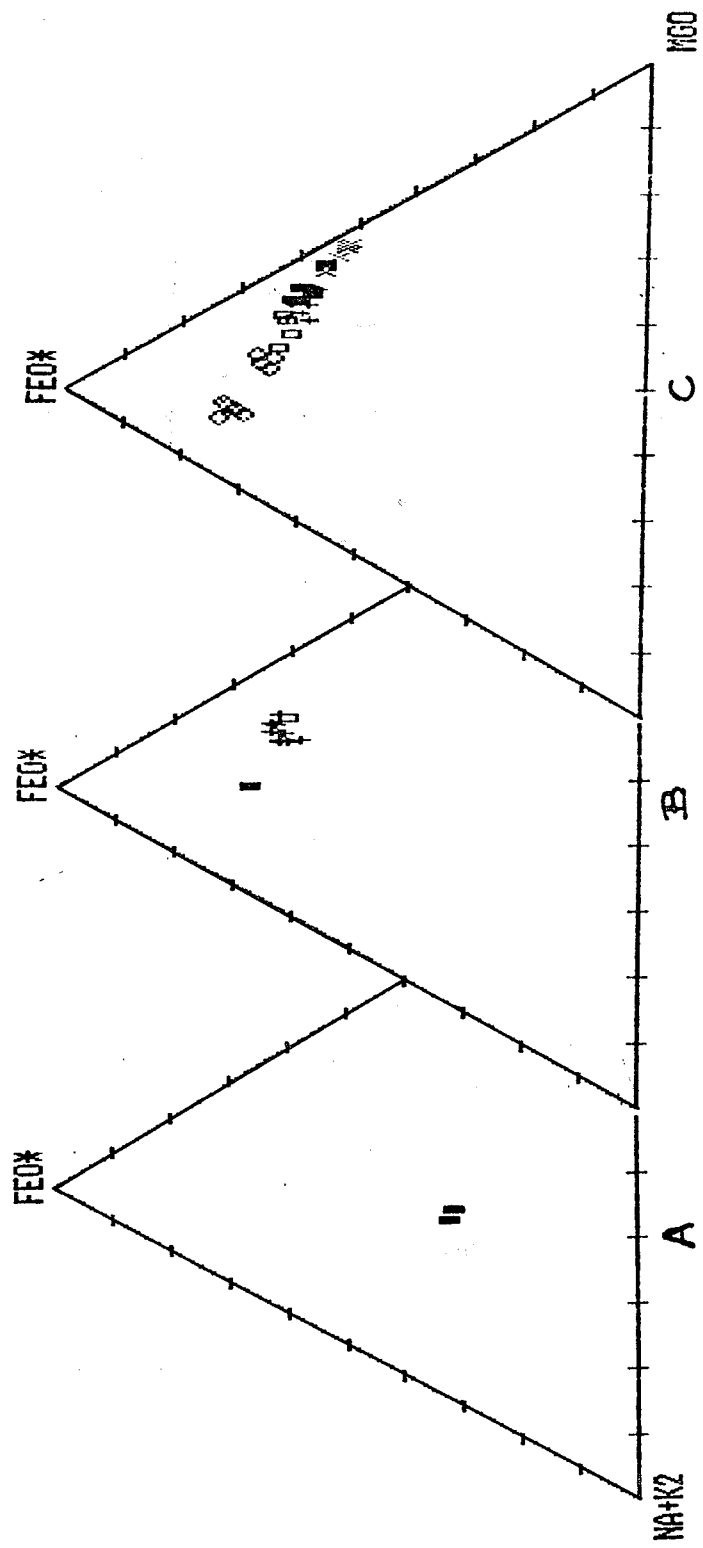


Fig. 13

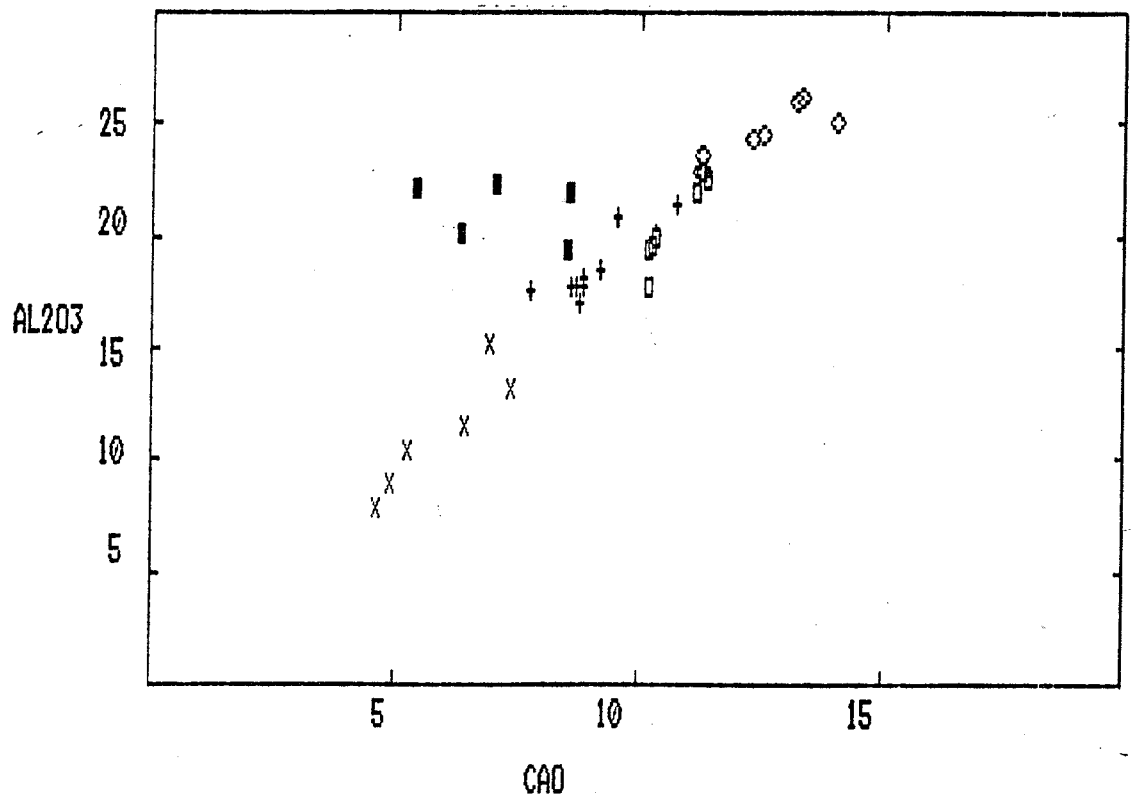
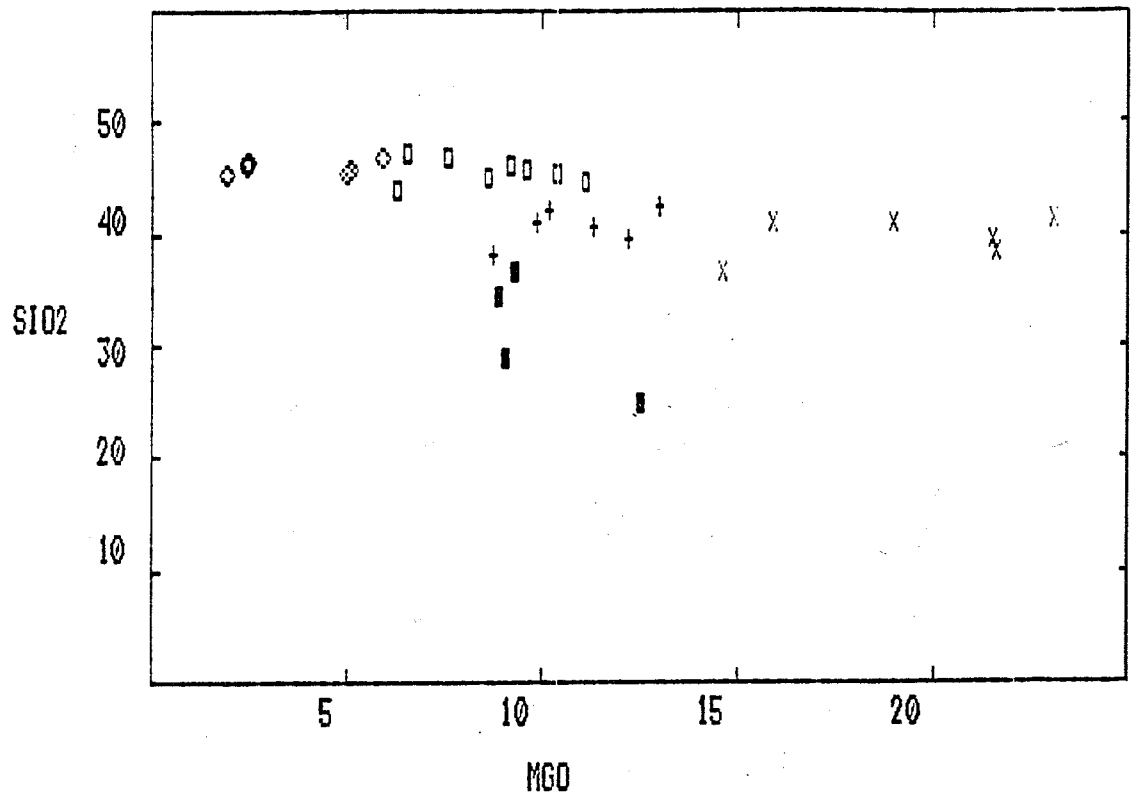


Fig. 14

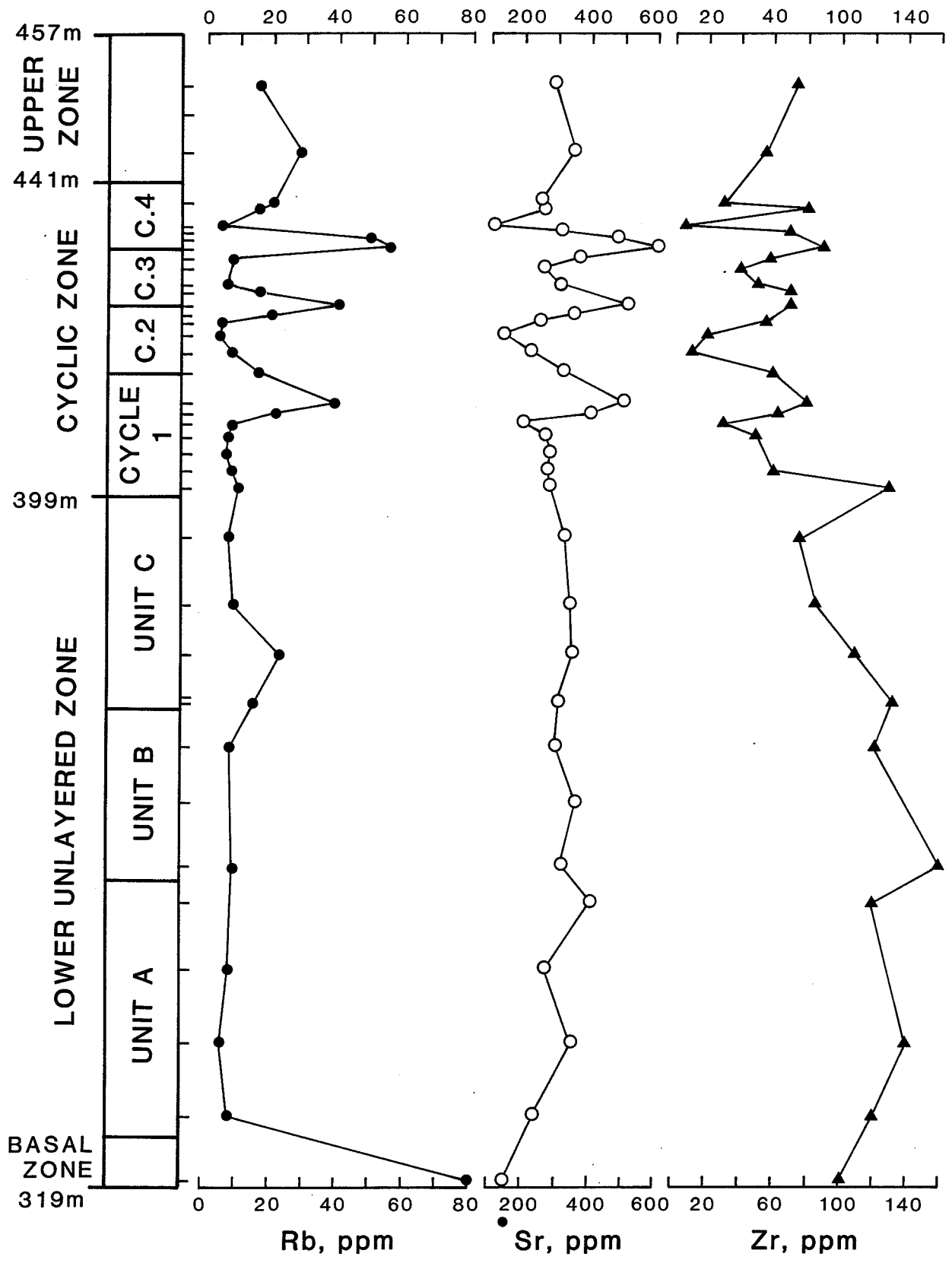


Fig. 15

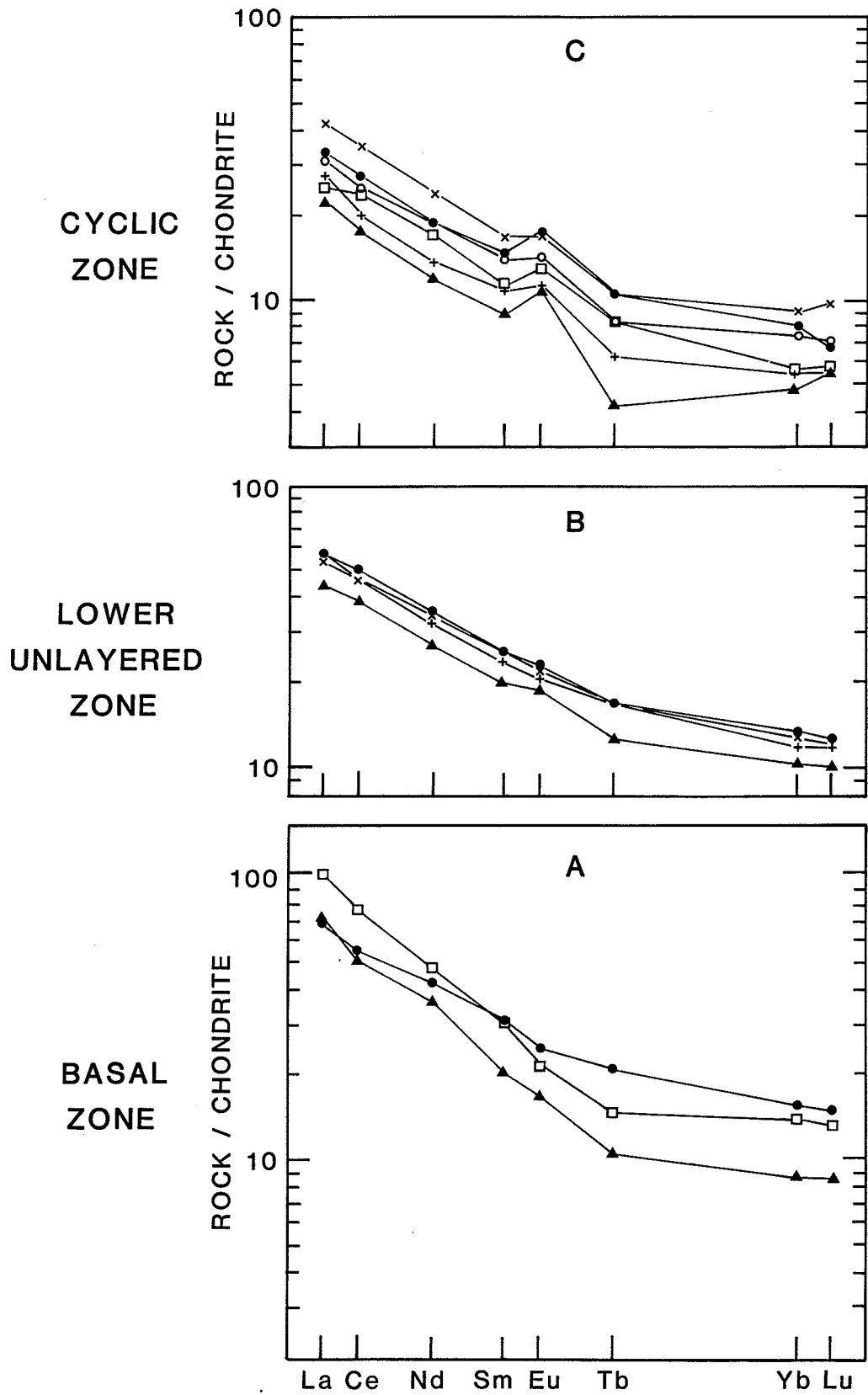


Fig. 16

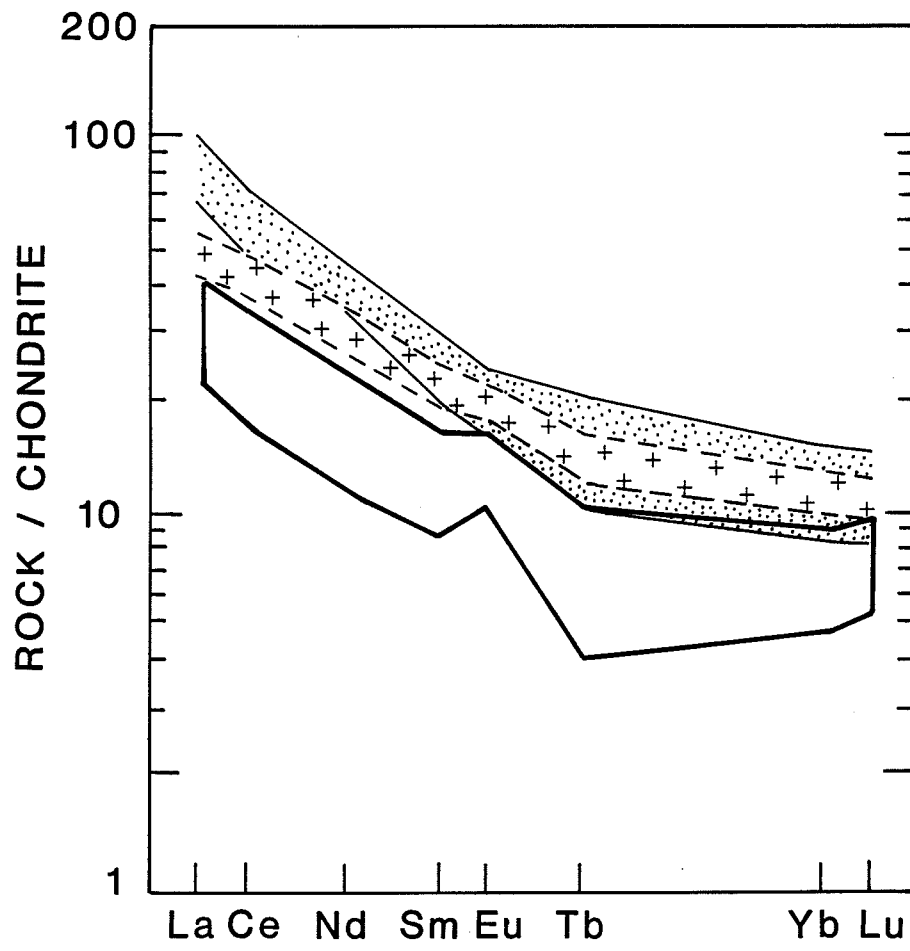
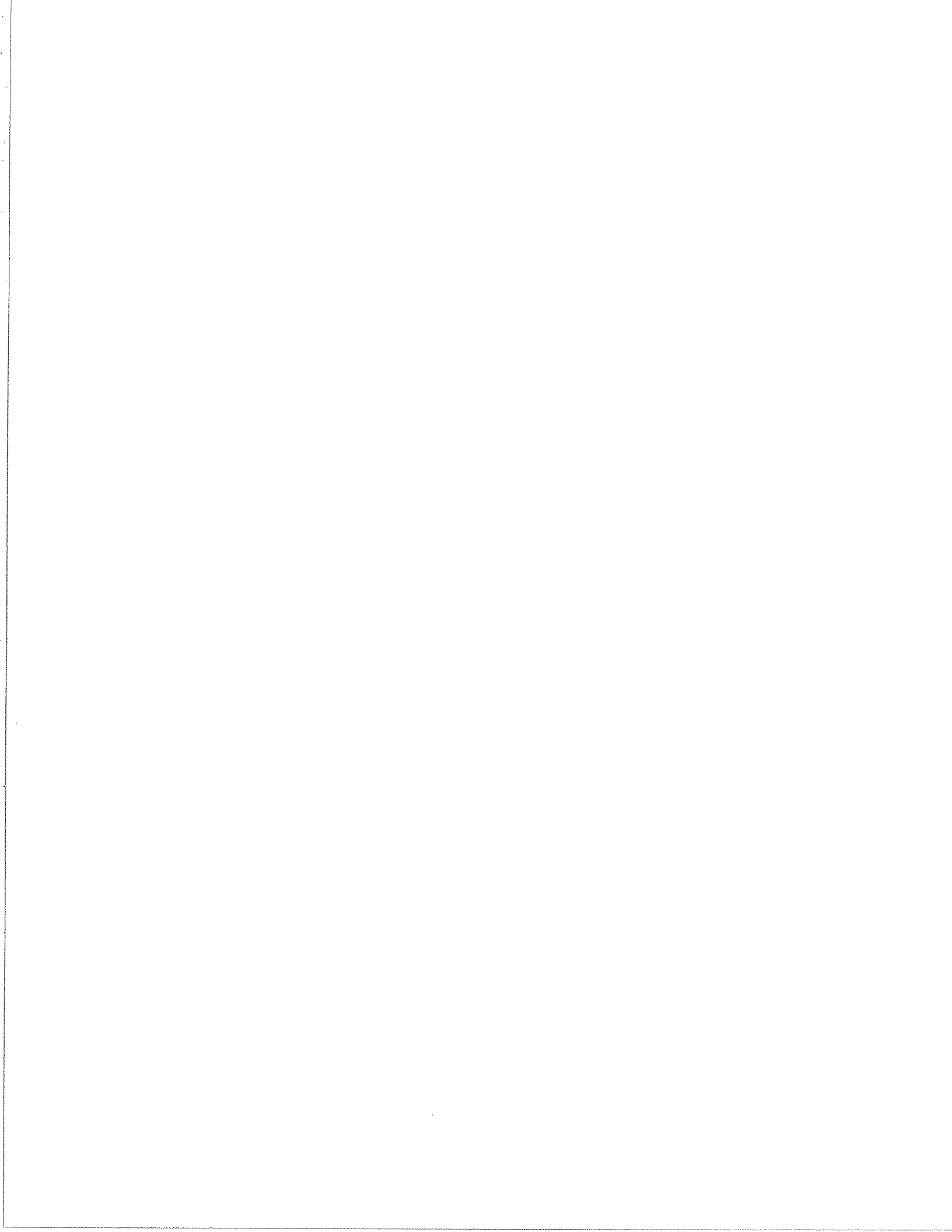


Fig. 17



PHOTOGRAPHS

Photo 1. Olivine gabbro, Cyclic zone. Patchy zoned plagioclase core is surrounded by normally zoned plagioclase margin. Augite contains eutectoid-like sulphide inclusions. Magnification x12. Sample 240-1.

Photo 2. Olivine gabbro, Cyclic zone. Olivine appears to resorb patchy and normally zoned plagioclase. Magnification x12. Sample 240-1.

Photo 3. Chrome spinel bearing orthocumulate gabbro, Cyclic zone. Normally zoned plagioclase, olivine, and augite, all with chrome spinel inclusions. Crossed nicols, magnification x12. Sample 252.

Photo 4. Same as photo 3, plane-polarized light.

Photo 5. Olivine gabbro, Unit A, Lower zone. Olivine and augite interstitial to plagioclase. Plane-polarized light, magnification x6. Sample DH18-147.

Photo 6. Fine- and coarse-grained olivine gabbro, Unit A, Lower zone. Poikilitic olivine appears to resorb plagioclase. Crossed nicols, magnification x6. Sample DH18-160.

Photo 7. Fine grained olivine gabbro at the base of the Unit A, Lower zone. Rounded to irregular olivine intergrowth within plagioclase. Crossed nicols, magnification x32. Sample DH18-184.

Photo 8. Medium grained olivine gabbro, Unit C, Lower zone. Upwardly branching skeletal olivine. Crossed nicols, magnification x6. Sample DH18-24.

Photo 9. Chrome spinel bearing cognate xenolith, Cycle 1, Cyclic zone. Chrome spinel and equant euhedral olivine is poikilitically included within plagioclase. Crossed nicols, magnification x11. Sample 244-2.

Photo 10. Chrome spinel free cognate xenolith, Cycle 2, Cyclic zone. Crossed nicols, magnification x11. Sample 243.

Photo 11. Chrome spinel bearing orthocumulate gabbro, Cycle 3, Cyclic zone. Olivine appears to resorb patchy zoned plagioclase and displays intergrowth texture with normally zoned plagioclase. Crossed nicols, magnification x11. Sample 267.

Photo 12. Chrome spinel bearing orthocumulate gabbro, Cycle 3, Cyclic zone. Poikilitic olivine contains numerous chrome spinel inclusions and plagioclase relicts. Crossed nicols, magnification x11. Sample 267.

Photo 13. Coarse-grained olivine gabbro, Unit C, Lower zone. Augite resorbs plagioclase. Crossed nicols, magnification x11. Sample 241.

Photo 14. Coarse grained olivine gabbro, Unit C, Lower zone. Augite contains plagioclase and olivine relicts. Crossed nicols, magnification x11. Sample 240.

Photo 15. Coarse grained gabbro, Unit A, Lower zone. Symplectite- to bleb-like intergrowth of orthopyroxene within plagioclase at the edge of olivine. Opaque ilmenite is partly surrounded by biotite. Crossed nicols, magnification x41. Sample DH18-160.

Photo 16. Chrome spinel bearing orthocumulate gabbro, Cycle 3, Cyclic zone. Augite, plagioclase and olivine containing chrome spinel inclusions. Chrome spinel grains within interstitial augite are irregular and larger than those in plagioclase cores and olivine. Crossed nicols, magnification x9. Sample 268.

TABLE 1

ROCK TYPES IN THE LOWER UNLAYERED (COPPER-NICKEL) ZONE

ROCK TYPE	CUMULATE TYPE	OCCURRENCE
Olivine gabbro	Plagioclase-olivine orthocumulate	Present in all units
Pegmatite	Plagioclase orthocumulate	Irregular patches, increasing in abundance upwards

XENOLITHS IN THE LOWER UNLAYERED (COPPER-NICKEL) ZONE

TYPE	ROCK TYPE	OCCURRENCE
Cognate	Olivine gabbro, fine-grained, plagioclase-olivine orthocumulate	Sparse, abundant in unit C
Sedimentary	Hornfels	Abundant in basal zone

TABLE 2

ROCK TYPES IN THE CYCLIC ZONE

ROCK TYPE	CUMULATE TYPE	CHROME SPINEL -BEARING
Troctolite	Cr-spinel poikilitic adcumulate	yes
Augite troctolite	Olivine-cr-spinel poikilitic adcumulate	yes
Olivine gabbro	Olivine-cr-spinel poikilitic orthocumulate	yes
	Plagioclase-olivine-cr-spinel poikilitic orthocumulate	yes
Olivine gabbro	Plagioclase-olivine ortho- cumulate	no
Anorthositic gabbro	Plagioclase orthocumulate	no
Pegmatitic olivine gabbro	Plagioclase orthocumulate	no

XENOLITHS IN THE CYCLIC ZONE

TYPE	ROCK TYPE	CHROME SPINEL -BEARING
Troctolite	Cr-spinel poikilitic adcumulate	yes
Augite troctolite	Olivine-Cr-spinel poikilitic adcumulate	yes
Olivine gabbro	Plagioclase-olivine orthocumulate	no

TABLE 3

STRUCTURAL CHARACTERISTICS OF THE CYCLIC UNITS

CYCLE 1	CYCLE 2	CYCLE 3	CYCLE 4
Poorly developed layering	Poorly developed layering	Beginning of visible layers	Well developed layering
Cr-spinel dissemination, layers and seams	Cr-spinel layers and seams	Three Cr-spinel layers and minor seams	Seven Cr-spinel layers
Trough bands	Planar lamination		Trough bands
Cognate xenoliths	Cognate xenoliths	Cognate xenoliths	
Fluid escape, load casts, drop and sag structures. Large sags filled with Cr-spinel disseminations	Slumped blocks, fluid escape, load casts, drop and sag structures	Drop and sag, fluid escape, load cast structures	Load casts, fluid escape structures

TABLE 4. COMPOSITIONS OF AUGITES IN THE BASAL ZONE

	208133	208134	208135	208238	MEAN
SiO2	48.85	49.95	49.75	49.00	49.39
TiO2	1.78	0.97	1.23	1.64	1.41
Al2O3	3.28	2.15	2.60	3.37	2.85
Cr2O3	0.09	0.09	0.08	0.11	0.09
FeO	12.79	16.09	14.30	12.99	14.04
MnO	0.30	0.42	0.33	0.31	0.34
MgO	12.68	12.74	13.22	13.13	12.94
CaO	19.58	17.71	18.54	19.77	18.90
Na2O	0.18	nd	0.07	0.24	0.16
K2O	0.07	0.09	0.03	0.05	0.06
Fe	21.15	26.16	23.20	21.05	22.89
Mg	37.38	36.93	38.25	37.92	37.62
Ca	41.47	36.90	38.56	41.03	39.49
TOTAL	99.60	100.21	100.15	100.61	100.18
Mg#	63.81	58.50	62.21	64.24	62.19

208133 - DH18-208 FINE GRAINED BASAL GABBRO
 208134 - DH18-208 FINE GRAINED BASAL GABBRO
 208135 - DH18-208 FINE GRAINED BASAL GABBRO
 208238 - DH18-208 FINE GRAINED BASAL GABBRO
 MEAN - MEAN OF ANALYSED AUGITES

TABLE 5. COMPOSITIONS OF DIFFERENT BIOTITES IN THE BASAL ZONE

	1	2	3	MEAN-1	4	5	6	7	MEAN-2
SiO ₂	37.87	40.23	39.18	39.09	35.34	35.68	38.07	36.62	36.43
Al ₂ O ₃	15.76	12.96	12.68	13.80	14.14	14.21	12.73	12.93	13.50
TiO ₂	3.47	1.88	3.25	2.87	4.57	4.31	4.03	4.58	4.37
Cr ₂ O ₃	0.42	0.39	0.36	0.39	0.27	0.27	0.10	0.12	0.19
FeO	11.35	13.26	14.82	13.14	24.35	24.20	18.21	21.68	22.11
MnO	nd	0.06	0.19	0.13	0.08	0.07	0.08	0.08	0.08
MgO	17.50	18.84	17.07	17.80	8.35	8.58	13.84	10.74	10.38
CaO	0.12	0.17	0.14	0.14	0.27	0.19	0.04	0.07	0.14
Na ₂ O	0.64	nd	0.12	0.38	0.67	0.10	0.35	0.40	0.38
K ₂ O	8.59	9.61	8.93	9.04	8.90	8.64	9.13	8.86	8.88
Fe	26.58	28.18	32.62	29.13	61.51	60.89	42.41	52.99	54.45
Mg	73.06	71.34	66.99	70.46	37.62	38.48	57.46	46.79	45.09
Ca	0.36	0.47	0.40	0.41	0.87	0.63	0.13	0.22	0.46
Mg#	72.90	71.36	66.96	70.41	37.82	38.61	57.50	46.86	45.47
TOTAL	95.72	97.40	96.74	96.78	96.94	96.25	96.58	96.08	96.46

- 1 - FINE GRAINED BASAL GABBRO 200-484-28
- 2 - FINE GRAINED BASAL GABBRO 303-2596-76
- 3 - FINE GRAINED BASAL GABBRO 303-2596-75
- MEAN-1 - MEAN OF BIOTITES EPITACTIC TO AUGITES
- 4 - FINE GRAINED BASAL GABBRO 200-284-41
- 5 - FINE GRAINED BASAL GABBRO 200-484-42
- 6 - FINE GRAINED BASAL GABBRO 303-2596-61
- 7 - FINE GRAINED BASAL GABBRO 303-2596-101
- MEAN-2 - MEAN OF BIOTITES ASSOCIATED WITH FELSIC MATERIAL

TABLE 6. ANALYSES OF OLIVINES IN THE LOWER UNLAYERED ZONE
(NUMBERS IN BRACKETS REPRESENT AVERAGED ANALYSES)

	1(12)	2(6)	3(15)	4(6)	5(13)	6(20)	7(9)	8(6)	9(7)	10(8)
SiO2	34.97	35.26	36.29	37.11	35.80	36.86	35.29	35.96	36.03	37.33
TiO2	0.09	0.14	0.09	0.11	0.10	0.07	0.09	0.09	nd	0.12
Al2O3	0.82	0.58	0.58	0.50	0.57	0.72	0.55	0.48	nd	0.44
Cr2O3	0.08	0.04	0.06	0.06	0.07	0.08	0.06	0.08	nd	0.04
FeO	38.13	32.33	31.25	32.43	33.09	30.20	36.99	35.30	30.83	28.39
MnO	0.68	0.70	0.40	0.31	0.63	0.59	0.91	0.57	0.52	0.40
MgO	24.88	30.22	30.48	30.89	28.68	31.50	25.83	28.14	31.23	33.47
CaO	0.16	0.13	0.20	0.19	0.20	0.14	0.10	0.14	0.21	0.02
Na2O	nd	nd	nd	nd	nd	nd	nd	nd	nd	nd
K2O	nd	nd	nd	nd	nd	nd	nd	nd	nd	nd
TOTAL	99.81	100.40	99.35	101.60	99.14	100.16	99.82	100.76	98.84	100.21
Mg#	53.80	62.53	63.51	62.96	60.73	65.04	55.48	58.72	64.41	67.79

- 1(12) - MEAN OF OLIVINES IN DH18-184 BASE OF THE UNIT A
- 2(6) - MEAN OF OLIVINES IN DH18-171 UNIT A
- 3(15) - MEAN OF OLIVINES IN DH18-160 UNIT A
- 4(6) - MEAN OF OLIVINES IN DH18-147 UNIT A
- 5(13) - MEAN OF OLIVINES IN DH18-125 UNIT A
- 6(20) - MEAN OF OLIVINES IN DH18-80 BASE OF THE UNIT B
- 7(9) - MEAN OF OLIVINES IN DH18-48 UPPER PORTION OF THE UNIT B
- 8(6) - MEAN OF OLIVINES IN DH18-24 LOWER PORTION OF THE UNIT C
- 9(7) - MEAN OF OLIVINES IN SAMPLE 25 UNIT C
- 10(8) - MEAN OF OLIVINES IN SAMPLE 241-2 UPPER PORTION OF THE UNIT C

TABLE 7. ANALYSES OF AUGITES IN THE LOWER UMLAYERED ZONE
(NUMBERS IN BRACKETS REPRESENT AVERAGED ANALYSES)

	1(5)	2(4)	3(5)	4(10)	5(6)	6(3)	7(8)	8(8)	9(6)	10(5)
SiO ₂	50.22	50.90	50.13	50.94	50.24	50.21	50.96	50.57	51.71	49.58
TiO ₂	1.16	1.28	1.19	1.16	1.18	0.88	1.03	1.38	1.16	1.07
Al ₂ O ₃	2.95	2.78	2.50	2.52	2.56	1.96	2.21	3.04	2.31	2.26
Cr ₂ O ₃	0.26	0.19	0.13	0.21	0.20	0.08	0.10	0.18	0.17	0.23
FeO	11.90	10.90	12.94	10.82	11.62	14.69	12.98	10.65	9.84	16.30
MnO	0.30	0.25	0.28	0.23	0.28	0.37	0.28	0.21	0.20	0.35
MgO	14.50	15.09	14.11	15.43	14.67	13.12	14.24	15.11	16.06	11.77
CaO	18.67	19.20	18.59	18.92	18.75	18.43	18.53	19.40	19.12	18.12
Na ₂ O	0.12	0.22	0.35	0.29	0.22	nd	0.14	0.05	nd	0.12
K ₂ O	0.08	0.07	0.06	0.05	0.06	0.05	0.05	0.06	0.06	0.04
Fe	19.30	17.45	20.90	17.29	18.80	23.81	20.90	17.06	15.64	27.00
Mg	41.91	43.11	40.64	43.96	42.31	37.92	40.88	43.12	45.47	34.67
Ca	38.79	39.44	38.47	38.76	38.89	38.27	38.22	39.82	38.90	38.36
Mg#	68.29	71.00	65.97	71.58	69.04	61.41	66.11	71.49	74.26	56.16
TOTAL	100.16	100.88	100.28	100.57	99.78	98.79	100.52	100.65	100.63	99.84

- 1(5) - MEAN OF AUGITES IN DH18-184 BASE OF THE UNIT A
- 2(4) - MEAN OF AUGITES IN DH18-171 UNIT A
- 3(5) - MEAN OF AUGITES IN DH18-109 UPPER PORTION OF THE UNIT A
- 4(10) - MEAN OF AUGITES IN DH18-80 BASE OF THE UNIT B
- 5(6) - MEAN OF AUGITES IN DH18-66 UNIT B
- 6(3) - MEAN OF AUGITES IN DH18-48 UPPER PORTION OF THE UNIT B
- 7(8) - MEAN OF AUGITES IN DH18-24 LOWER PORTION OF THE UNIT C
- 8(8) - MEAN OF AUGITES IN 241-1 UNIT C
- 9(6) - MEAN OF AUGITES IN 241-2 UPPER PORTION OF THE UNIT C
- 10(5) - MEAN OF AUGITES CONTAINING SULPHIDE INCLUSIONS DH18-160 UNIT A

TABLE 8. MINERAL COMPOSITIONS IN PEGMATITIC GABBROS AND COGNATE XENOLITHS. (NUMBERS IN BRACKETS REPRESENT AVERAGED ANALYSES)

	1(20)	2(13)	3(2)	4(5)	5(6)	6(10)
SI02	35.54	49.27	39.03	36.67	35.29	49.33
TIO2	nd	2.26	3.11	4.61	nd	3.44
AL2O3	nd	1.23	12.39	11.77	nd	1.24
CR2O3	nd	0.18	0.10	0.15	nd	0.20
FEO	35.71	12.49	10.63	22.25	35.47	12.09
MNO	0.52	0.30	0.11	0.14	0.62	0.21
MGO	28.56	13.69	19.34	10.86	27.76	13.99
CAO	0.37	18.87	0.12	0.13	0.21	18.45
NA2O	nd	0.50	1.04	0.52	nd	0.96
K2O	nd	0.17	8.13	8.64	nd	0.39
TOTAL	100.70	98.96	94.00	95.74	99.35	100.30

- 1(20) - MEAN OF OLIVINES IN PEGMATITIC GABBRO SAMPLE 241 UNIT C
- 2(13) - MEAN OF AUGITES IN PEGMATITIC GABBRO SAMPLE 241 UNIT C
- 3(2) - MEAN OF BIOTITES EPITACTIC TO OLIVINE IN PEGMATITIC GABBRO 241 UNIT C
- 4(5) - MEAN OF BIOTITES EPITACTIC TO AUGITE IN PEGMATITIC GABBRO 241 UNIT C
- 5(6) - MEAN OF OLIVINES IN FINE GRAINED COGNATE XENOLITH SAMPLE 24 UNIT C
- 6(10) - MEAN OF AUGITES IN FINE GRAINED COGNATE XENOLITH SAMPLE 24 UNIT C

TABLE 9. COMPOSITIONS OF OLIVINES IN THE CYCLIC UNITS
(NUMBERS IN BRACKETS REPRESENT AVERAGED ANALYSES)

	1(12)	2(5)	3(14)	4(13)	5(13)	6(10)
SiO ₂	38.87	38.93	37.50	37.28	37.29	36.75
MgO	42.07	38.71	36.27	35.25	33.13	33.05
FeO	18.11	22.55	25.00	26.12	29.73	30.11
MnO	0.32	0.42	0.31	0.31	0.42	0.42
CaO	0.05	0.11	0.16	0.16	0.16	0.16
NiO	0.17	0.17	0.33	0.17	0.17	nd
TOTAL	99.59	100.89	99.57	99.29	100.90	100.49
FO	80.55	75.35	72.11	70.65	66.52	66.18
FA	19.45	24.65	27.89	29.35	33.48	33.82

- 1(12) - MEAN OF OLIVINES IN CHROME-SPINEL ADCUMULATE 14-2 CYCLE 4
 2(5) - MEAN OF OLIVINES IN DISRUPTED CHROME-SPINEL ADCUMULATE 246 CYCLE 1
 3(14) - MEAN OF EQUEDRAL OLIVINES IN OLIVINE-CHROME SPINEL ORTHOCUMULATE 2588 CYCLE
 4(13) - MEAN OF POIKILITICAL OLIVINES IN CHROME-SPINEL ORTHOCUMULATE 271-1 CYCLE 3
 5(13) - MEAN OF INTERSTITIAL OLIVINES IN CHROME-SPINEL ORTHOCUMULATE 268 CYCLE 3
 6(10) - MEAN OF SKELETAL OLIVINES IN ANORTHOSITIC GABBRO 248 CYCLE 1

TABLE 10. COMPOSITIONS OF AUGITES, ORTHOPYROXENES, AND HORNBLENDES IN THE CYCLIC ZONE. (NUMBERS IN BRACKETS REPRESENT AVERAGED ANALYSES)

	1(7)	2(8)	3(8)	4(11)	5(5)	6(4)	7(4)	8(6)
SiO ₂	49.98	50.47	50.68	50.48	43.96	48.21	54.09	52.04
Al ₂ O ₃	2.88	2.47	2.49	2.34	9.18	7.20	1.05	0.90
TiO ₂	1.16	1.00	1.05	1.13	3.20	1.90	0.51	0.41
Cr ₂ O ₃	0.94	0.73	0.26	0.24	0.20	0.64	0.20	0.09
FeO	7.97	8.93	10.91	9.53	12.75	8.91	15.66	21.41
MnO	0.19	0.24	0.23	0.18	0.11	0.22	0.35	0.37
MgO	15.66	15.72	14.37	15.46	14.67	17.34	27.77	23.14
CaO	20.26	19.74	19.66	19.87	11.78	12.46	1.63	1.73
Na ₂ O	0.40	0.55	0.03	0.28	2.84	2.00	0.31	0.29
K ₂ O	0.04	0.06	0.07	0.05	1.00	0.40	0.04	0.05
Fe	12.89	14.34	17.64	15.24	23.62	15.97	23.32	33.02
Mg	45.12	45.03	41.52	44.05	48.43	55.39	73.58	63.58
Ca	41.99	40.63	40.80	40.71	27.95	28.64	3.10	3.41
TOTAL	99.48	99.91	99.75	99.56	99.69	99.28	101.62	100.43

- 1(7) - MEAN OF AUGITES IN OLIVINE-CHROME SPINEL ADCUMULATE 244 CYCLE 1
 2(8) - MEAN OF AUGITES IN FLAG-OL-CR.SPINEL ORTHOCUMULATE 252 CYCLE 2
 3(8) - MEAN OF AUGITES WHICH CONTAIN SULPHIDE INCLUSIONS 240-1 CYCLE 1
 4(11) - MEAN OF AUGITES IN ANORTHOSITIC GABBRO 248 AND 251 CYCLE 1
 5(5) - MEAN OF HORNBLENDES IN FLAG-OLIV ORTHOCUMULATE 240-1 CYCLE 1
 6(4) - MEAN OF HORNBLENDES IN CHROME-SPINEL ORTHOCUMULATE 252.CYCLE 2
 7(4) - MEAN OF ORTHOPYROXENES EPITACTIC TO OLIVINES 252 AND 261 CYCLE 2
 8(6) - MEAN OF ORTHOPYROXENES EPITACTIC TO AUGITES IN ORTHOCUMULATES 241-3 AND 248

TABLE 11. ANALYSES OF BIOTITES IN THE CYCLIC ZONE
(NUMBERS IN BRACKETS REPRESENT AVERAGED ANALYSES)

	1(5)	2(5)	3(8)	4(13)
SiO ₂	36.14	38.27	38.51	37.03
Al ₂ O ₃	13.49	12.75	13.12	12.68
TiO ₂	5.78	6.28	5.02	5.02
Cr ₂ O ₃	0.98	1.13	0.64	0.42
FeO	6.26	11.95	9.53	15.08
MnO	nd	0.11	0.11	0.15
MgO	19.37	16.22	18.75	15.85
CaO	0.12	0.15	0.18	0.20
Na ₂ O	1.48	0.63	0.80	0.48
K ₂ O	7.57	8.99	8.54	7.97
Fe	15.29	29.12	22.10	34.45
Mg	84.46	70.41	77.36	64.96
Ca	0.37	0.48	0.53	0.59
TOTAL	91.19	96.48	95.20	94.88

- 1(5) - MEAN OF BIOTITES IN CHROME-SPINEL ADCUMULATE 14-2 CYCLE 4
 2(5) - MEAN OF BIOTITES IN DISRUPTED CHROME-SPINEL ADCUMULATE 246 CYCLE 1
 3(8) - MEAN OF BIOTITES EPITACTIC TO OLIVINE IN ORTHOCUMULATES CYCLES 1-4
 4(13) - MEAN OF BIOTITES EPITACTIC TO AUGITE IN ORTHOCUMULATES CYCLES 1-4

TABLE 12. MAJOR AND TRACE ELEMENT ANALYSES OF GABBROS IN
THE BASAL ZONE

	223*	517
SiO ₂	47.50	53.00
Al ₂ O ₃	18.90	14.40
Fe ₂ O ₃	12.10	18.00
MgO	5.82	3.08
CaO	1.09	0.86
Na ₂ O	1.06	1.73
K ₂ O	6.68	2.84
TiO ₂	1.13	1.47
P ₂ O ₅	0.09	0.15
MnO	0.09	0.09
S	nd	nd
BA PPM	nd	nd
CR	270	170
ZR	100.00	100.00
SR	150	100.00
RB	80.00	10.00
Y	10.00	30.00
NB	10.00	20.00
ZN	nd	nd
NI	nd	nd
LOI	4.77	3.85
TOTAL	99.30	99.50
NA+K ₂	7.74	4.57
FeO*	6.33	3.63

223* - FINE GRAINED BASAL GABBRO DH18
517 - FINE GRAINED BASAL GABBRO DH201

TABLE 13. MAJOR AND TRACE ELEMENT DATA FOR GABBROS OF
THE LOWER UNLAYERED ZONE

	24*	240	241.1	241.2	25	48*	60*	95*	125*	160*	184*	2400
SiO2	46.00	47.22	46.70	46.91	46.21	48.70	46.00	44.00	44.30	45.20	46.70	45.75
Al2O3	18.40	18.58	21.29	20.99	20.87	19.70	17.20	18.50	17.90	17.70	16.90	19.21
Fe2O3T	12.50	11.15	9.96	9.48	9.72	9.83	13.00	12.70	13.90	14.20	13.20	12.28
MgO	7.00	7.01	7.45	8.95	8.12	3.46	6.17	6.62	7.22	6.16	6.86	3.83
CaO	9.24	10.52	10.91	10.69	11.03	11.20	8.87	8.06	9.64	9.44	9.39	9.86
Na2O	2.44	2.71	2.42	2.23	2.31	2.71	2.41	1.95	2.03	2.13	2.20	2.43
K2O	0.58	0.62	0.49	0.28	0.35	0.87	0.73	1.42	0.51	0.92	0.67	0.38
TiO2	1.32	1.65	1.04	0.92	0.92	1.83	1.90	1.35	1.48	1.78	1.74	1.06
P2O5	0.21	0.05	nd	nd	nd	0.29	0.25	0.18	0.17	0.20	0.21	nd
MnO	0.14	0.14	0.12	0.12	0.12	0.13	0.16	0.14	0.15	0.14	0.16	0.15
S	nd	0.01	0.03	0.02	0.01	nd	nd	nd	nd	nd	nd	0.02
BA	nd	193	141	115	150	nd	nd	nd	nd	nd	nd	129
CR	70.00	169	187	174	211	100.00	130	170	170	150	160	205
ZR	120	134	87.00	76.00	72.00	180	160	120	70.00	140	120	85.00
						"						
SR	300	307	344	322	335	360	320	410	270	350	240	290
RB	10.00	15.00	9.00	1.00	9.00	10.00	10.00	10.00	10.00	10.00	1020	4.00
Y	20.00	33.00	25.00	21.00	18.00	30.00	20.00	10.00	10.00	10.00	20.00	23.00
NB	20.00	7.00	5.00	6.00	2.00	20.00	20.00	20.00	20.00	30.00	nd	5.00
ZN	nd	90.00	72.00	74.00	80.00	nd	nd	nd	nd	nd	nd	93.00
NI	nd	227	337	312	276	nd	nd	nd	nd	nd	nd	368
LOI	.77000	nd	nd	nd	nd	.77000	2.16	3.39	.85000	.54000	.77000	nd
NA+K2	3.02	3.33	2.91	2.51	2.66	3.58	3.14	3.37	2.54	3.05	2.87	2.81
TOTAL	98.70	99.80	100.57	100.71	99.81	99.60	98.90	98.40	98.20	98.50	98.90	100.09
FeO#	15.54	16.83	17.62	18.74	18.34	14.31	14.42	14.02	16.14	14.98	15.56	17.81

- 24* - UNIT C.MEDIUM GRAINED OLIVINE GABBRO
- 240 - UNIT.C MEDIUM GRAINED OLIVINE GABBRO
- 241.1 - UNIT.C.MEDIUM GRAINED OLIVINE GABBRO
- 241.2 - UNIT C.MEDIUM GRAINED OLIVINE GABBRO
- 25 - UNIT C.FINE TO MEDIUM GRAINED OLIVINE GABBRO
- 48* - UNIT B.CONTAMINATED MEDIUM GRAINED OLIVINE GABBRO
- 60* - UNIT B.MEDIUM GRAINED OLIVINE GABBRO
- 95* - UNIT A.FINE TO MEDIUM GRAINED OLIVINE GABBRO
- 125* - UNIT A.FINE TO MEDIUM GRAINED OLIVINE GABBRO
- 160* - UNIT A.FINE TO MEDIUM GRAINED OLIVINE GABBRO
- 184* - UNIT A.FINE GRAINED OLIVINE GABBRO
- 24COG - FINE GRAINED COGNATE XENOLITH.UNIT C.

TABLE 14. MAJOR AND TRACE ELEMENT ANALYSES OF ADCUMULATE XENOLITHS AND SLUMPED FINE GRAINED GABBROS

	244	258	244*	255*	258A*	257*
SiO2	38.42	40.82	39.60	41.30	41.00	34.40
Al2O3	10.51	11.56	9.00	7.93	13.20	21.90
Fe2O3T	17.71	16.06	18.10	18.30	14.40	15.80
MgO	21.61	18.98	21.50	23.10	15.90	8.90
CaO	5.25	6.43	4.89	4.59	7.35	8.52
Na2O	1.12	1.24	0.77	0.85	1.30	1.35
K2O	0.16	0.18	0.20	0.20	0.24	0.22
TiO2	0.85	0.82	0.83	0.81	0.96	1.54
P2O5	nd	nd	0.08	0.11	0.10	0.06
MnO	0.21	0.19	0.22	0.24	0.17	0.15
S	0.06	0.15	nd	nd	nd	nd
BA	56.00	53.00	nd	nd	nd	nd
CR	13081	4513	9330	3320	4410	43300
ZR	36.00	48.00	30.00	50.00	40.00	20.00
SR	120	143	90.00	80.00	160	190
RB	4.00	5.00	20.00	10.00	10.00	10.00
Y	15.00	20.00	10.00	10.00	10.00	10.00
NB	3.00	1.00	20.00	30.00	20.00	20.00
ZN	178	140	nd	nd	nd	nd
NI	1045	2153	nd	nd	nd	nd
LOI	nd	nd	2.62	2.23	1.70	.62000
FeO*	24.70	23.51	24.24	25.38	21.66	16.53
Na+K2	1.28	1.42	.97000	1.05	1.54	1.57
TOTAL	97.98	97.39	99.20	100.00	97.00	99.80

- 244 - OL-CR.SPINEL POIKILITICAL ADCUMULATE XENOLITH CYCLE 1
- 258 - FINE GRAINED SLUMPED ROCK CYCLE 2
- 244* - OL-CR.SPINEL POIKILITICAL ADCUMULATE XENOLITH CYCLE 1
- 255* - OL-CR.SPINEL POIKILITICAL ADCUMULATE XENOLITH CYCLE 2
- 258A* - FINE GRAINED SLUMPED ROCK CYCLE 2
- 257* - CHROME SPINEL ADCUMULATE XENOLITH CYCLE 2

TABLE 15. MAJOR AND TRACE ELEMENT DATA FOR CHROME SPINEL
ADCUMULATE ROCKS

	14*	245*	246*	254*
SiO2	24.80	39.30	36.60	29.00
Al2O3	22.20	20.50	19.30	22.30
Fe2O3T	18.00	13.00	14.40	18.00
MgO	12.50	8.09	9.28	9.06
CaO	5.40	9.49	8.51	7.04
Na2O	0.86	1.57	1.47	1.07
K2O	0.22	0.44	0.30	0.20
TiO2	1.23	1.42	1.43	1.52
P2O5	0.05	0.09	0.07	0.06
MnO	0.18	0.14	0.16	0.16
S	nd	nd	nd	nd
BA	nd	nd	nd	nd
CR	88100	22400	26300	60900
ZR	10.00	50.00	30.00	20.00
SR	110.00	250	200	140
RB	10.00	10.00	10.00	10.00
Y	10.00	20.00	10.00	10.00
NB	30.00	20.00	30.00	10.00
ZN	nd	nd	nd	nd
NI	nd	nd	nd	nd
LOI	2.00	1.16	.77000	.93000
NA+K2	1.08	2.01	1.77	1.27
FEO*	16.65	16.77	16.86	15.19
TOTAL	100.30	98.50	96.20	98.30

- 14* - CHROME SPINEL POIKILITICAL ADCUMULATE LAYER CYCLE 4
245* - DISRUPTED CHROME SPINEL ADCUMULATE CYCLE 1
246* - DISRUPTED CHROME SPINEL ADCUMULATE CYCLE 1
254* - DISRUPTED CHROME SPINEL ADCUMULATE IN SLUMPED ROCKS CYCLE 2

TABLE 16. MAJOR AND TRACE ELEMENT DATA FOR CHROME-SPINEL
ORTHOCUMULATE ROCKS

	252	271	20*	252*	267*	271*
SiO2	42.47	40.51	39.10	38.00	41.90	41.10
Al2O3	17.06	17.77	18.50	17.80	17.80	18.10
Fe2O3T	13.07	14.52	15.00	15.80	13.50	13.80
MgO	13.00	11.29	6.84	8.77	10.20	9.86
CaO	8.76	8.68	9.17	8.83	8.57	8.83
Na2O	1.82	1.84	1.69	1.50	1.56	1.56
K2O	0.30	0.45	0.66	0.21	0.86	0.49
TiO2	1.31	1.33	2.27	2.03	1.27	1.36
P2O5	nd	nd	0.09	0.07	0.09	0.08
MnO	0.16	0.16	0.16	0.17	0.16	0.16
S	0.02	0.04	nd	nd	nd	nd
BA	170	89.00	nd	nd	nd	nd
CR	8909	14251	25100	26400	11700	17500
ZR	64.00	44.00	30.00	10.00	50.00	40.00
SR	225	268	250	180	310	260
RB	8.00	14.00	20.00	10.00	10.00	10.00
Y	18.00	13.00	10.00	10.00	10.00	10.00
NB	6.00	2.00	30.00	30.00	20.00	20.00
ZN	151	119	nd	nd	nd	nd
NI	647	479	nd	nd	nd	nd
LOI	nd	nd	1.00	.23000	.93000	.62000
Na+K2	2.12	2.29	2.35	1.71	2.42	2.05
FeO*	20.46	18.84	15.33	16.72	17.75	17.70
TOTAL	99.42	98.81	98.20	97.30	98.60	98.60

- 252 - CHROME SPINEL ORTHOCUMULATE CYCLE 2
- 271 - CHROME SPINEL ORTHOCUMULATE CYCLE 3
- 20* - CHROME SPINEL ORTHOCUMULATE LAYER CYCLE 4
- 252* - CHROME SPINEL ORTHOCUMULATE CYCLE 2
- 267* - CHROME SPINEL ORTHOCUMULATE CYCLE 3
- 271* - CHROME SPINEL ORTHOCUMULATE CYCLE 3

TABLE 17. MAJOR AND TRACE ELEMENT ANALYSES OF CHROME-SPINEL-FREE
ORTHOCUMULATE ROCKS

	242.2	242	264	266	268	270	273	278	19	21
SiO2	43.87	45.97	46.81	47.25	46.30	46.75	45.96	45.31	45.94	43.34
Al2O3	22.42	19.54	23.92	21.92	20.45	19.90	21.32	20.00	19.83	20.71
Fe2O3T	10.07	10.43	6.29	8.54	9.44	9.49	8.85	8.96	10.06	11.47
MgO	6.28	9.42	5.57	6.56	8.33	7.61	9.20	9.86	9.87	7.61
CaO	11.36	10.49	12.35	11.13	9.89	10.33	10.76	10.40	10.36	10.00
Na2O	2.14	2.40	2.40	2.61	2.29	2.39	2.24	2.16	2.25	2.37
K2O	0.40	0.27	0.50	0.66	1.07	0.83	0.42	0.46	0.42	0.78
TiO2	1.19	0.81	0.63	0.93	0.97	1.07	0.69	0.86	0.78	1.33
P2O5	nd	nd	nd	nd	0.01	nd	nd	nd	nd	nd
MnO	0.11	0.14	0.08	0.11	0.12	0.12	0.11	0.11	0.13	0.13
S	0.02	0.09	0.03	0.03	0.02	0.04	0.02	0.02	0.02	0.01
BA	107.00	104.00	132	132	218	201	58.00	81.00	140	144
CR	7406	234	397	83.00	221	270	220	1262	485	9460
ZR	60.00	59.00	53.00	70.00	84.00	90.00	57.00	70.00	72.00	55.00
SR	310	273	359	356	452	417	363	308	286	346
RB	6.00	6.00	12.00	16.00	39.00	27.00	9.00	16.00	11.00	29.00
Y	15.00	22.00	15.00	22.00	24.00	25.00	17.00	20.00	20.00	11.00
NB	3.00	4.00	nd	5.00	5.00	4.00	3.00	4.00	5.00	3.00
ZN	111	96.00	46.00	55.00	72.00	60.00	61.00	55.00	91.00	127
NI	306	517	205	202	297	240	321	366	380	301
LOI	nd	nd	nd	nd	nd	nd	nd	nd	nd	nd
NA+K2	2.54	2.67	2.90	3.27	3.36	3.22	2.66	2.62	2.67	3.15
FEO*	17.01	18.97	17.36	17.03	17.39	17.18	19.04	19.27	19.24	16.85
TOTAL	99.06	99.70	98.76	99.85	99.07	98.69	99.71	98.44	99.85	99.26

242.2 - PL-OL ORTHOCUMULATE CYCLE 1
 242 - PL-OL ORTHOCUMULATE CYCLE 1
 264 - PL-OL ORTHOCUMULATE CYCLE 3
 266 - PL-OL ORTHOCUMULATE CYCLE 3
 268 - PL-OL ORTHOCUMULATE CYCLE 3
 270 - PL-OL ORTHOCUMULATE CYCLE 3
 273 - PL-OL ORTHOCUMULATE CYCLE 3
 278 - PL-OL ORTHOCUMULATE CYCLE 4
 19 - PL-OL ORTHOCUMULATE CYCLE 4
 21 - PL-OL ORTHOCUMULATE CYCLE 4

TABLE 18. MAJOR AND TRACE ELEMENT DATA FOR ANORTHOSITIC GABBROS
IN THE CYCLIC ZONE

	249	262	275	276	13	262*	275*	276*
SiO ₂	46.90	46.31	46.26	45.80	44.78	46.50	46.40	45.50
Al ₂ O ₃	23.57	25.94	24.27	22.85	23.56	26.10	24.50	22.80
Fe ₂ O ₃ T	6.83	5.04	5.68	7.42	4.70	5.01	5.68	7.45
MgO	5.93	2.44	2.45	5.07	2.91	2.51	2.46	5.01
CaO	11.25	13.17	12.28	11.20	16.79	13.30	12.50	11.30
Na ₂ O	2.50	2.27	2.52	2.37	1.59	2.01	2.08	1.97
K ₂ O	0.93	1.28	1.62	1.13	1.25	1.34	1.66	1.16
TiO ₂	0.82	0.83	1.02	0.94	0.77	0.83	1.01	0.94
P ₂ O ₅	nd	nd	nd	nd	nd	0.11	0.14	0.13
MnO	0.09	0.07	0.08	0.10	0.09	0.06	0.07	0.09
S	0.02	0.02	0.01	0.02	0.01	nd	nd	nd
BA	108.00	366	267	196	551	nd	nd	nd
CR	135	418	2581	2029	603	490	3400	2560
ZR	78.00	70.00	96.00	79.00	71.00	50.00	90.00	60.00
SR	502	476	617	450	348	520	670	470
RB	39.00	43.00	58.00	44.00	38.00	40.00	60.00	50.00
Y	26.00	15.00	22.00	21.00	18.00	10.00	10.00	10.00
NB	7.00	4.00	6.00	4.00	4.00	10.00	20.00	10.00
ZN	82.00	43.00	62.00	68.00	30.00	nd	nd	nd
NI	208	83.00	69.00	163	61.00	nd	nd	nd
LOI	nd	nd	nd	nd	nd	2.08	2.47	2.47
Na+K ₂	3.43	3.55	4.14	3.50	2.84	3.35	3.74	3.13
FEO*	16.59	15.37	14.49	15.76	19.41	15.56	14.71	15.81
TOTAL	98.99	97.56	96.71	97.30	96.65	100.00	99.60	99.30

249 - ANORTHOSITIC GABBRO CYCLE 1
 262 - ANORTHOSITIC GABBRO CYCLE 2
 275 - ANORTHOSITIC GABBRO CYCLE 3
 276 - ANORTHOSITIC GABBRO CYCLE 3
 13 - ANORTHOSITIC GABBRO CYCLE 2
 262* - ANORTHOSITIC GABBRO CYCLE 2
 275* - ANORTHOSITIC GABBRO CYCLE 3
 276* - ANORTHOSITIC GABBRO CYCLE 3

TABLE 19. RARE EARTH CONCENTRATIONS OF GABBROS
IN THE BASAL ZONE

	1	2	3
LA	21.70	32.30	21.50
CE	40.00	61.00	44.00
ND	20.00	28.00	25.00
SM	3.74	5.66	5.86
EU	1.17	1.53	1.74
TB	0.50	0.70	1.00
YB	1.72	2.78	3.13
LU	0.26	0.41	0.46
TOTAL	89.09	132	102.69
LA/YB	12.60	11.60	6.86

- 1 - FINE GRAINED BASAL GABBRO DH18-223
- 2 - FINE GRAINED BASAL GABBRO 201-517
- 3 - FINE GRAINED BASAL GABBRO 141-2264

"

TABLE 20. RARE EARTH CONCENTRATIONS OF GABBROS
IN THE LOWER UNLAYERED ZONE

	1	2	3
LA	17.80	13.70	17.80
CE	40.00	31.00	37.00
ND	21.00	16.00	19.00
SM	4.81	3.72	4.43
EU	1.60	1.32	1.45
TB	0.80	0.60	0.80
YB	2.67	2.06	2.37
LU	0.39	0.31	0.36
TOTAL	89.07	68.71	83.21
LA/YB	6.66	6.65	7.51

- 1 - FINE GRAINED OLIVINE GABBRO DH18-184 UNIT A
 2 - MEDIUM GRAINED OLIVINE GABBRO DH18-125 UNIT A
 3 - MEDIUM GRAINED OLIVINE GABBRO DH18-24 UNIT C

TABLE 21. RARE EARTH CONCENTRATIONS OF GABBROS
IN THE CYCLIC ZONE

	1	2	3	4	5
LA	7.80	10.30	7.00	8.60	13.20
CE	19.00	22.00	14.00	16.00	28.00
ND	10.00	11.00	7.00	8.00	14.00
SM	2.12	2.73	1.67	2.04	3.14
EU	0.91	1.24	0.77	0.80	1.19
TB	0.40	0.50	0.20	0.30	0.50
YB	1.14	1.64	0.97	1.10	1.82
LU	0.18	0.21	0.17	0.17	0.30
TOTAL	41.55	49.62	31.78	37.01	62.15
LA/YB	6.84	6.28	7.21	7.81	7.25

- 1 - ANORTHOSITIC GABBRO 248 CYCLE 1
- 2 - ANORTHOSITIC GABBRO 251 CYCLE 1
- 3 - ANORTHOSITIC GABBRO 261 CYCLE 2
- 4 - OLIVINE GABBRO 273 CYCLE 3
- 5 - ANORTHOSITIC GABBRO 275 CYCLE 3

TABLE 22

REE in Zones of the Crystal Lake Intrusion

	<u>Total REE</u>	<u>Eu</u>	<u>La/Yb</u>
Cyclic zone	31.78-62.15	0.77-1.24	6.28-7.81
Lower unlayered zone	68.71-89.07	1.32-1.60	6.66-7.51
Basal zone	89.04-132.38	1.17-1.74	6.86-12.60

